NASA Technical Paper 1601

The Effects of Motion and g-Seat Cues on Pilot Simulator Performance of Three Piloting Tasks

Thomas W. Showalter and Benton L. Parris

JANUARY 1980

NASA

NASA Technical Paper 1601

The Effects of Motion and g-Seat Cues on Pilot Simulator Performance of Three Piloting Tasks

Thomas W. Showalter and Benton L. Parris
Ames Research Center
Moffett Field, California

NASA
National Aeronautics
and Space Administration

Scientific and Technical
Information Office

1980

SYMBOLS

A_i	attitude drive components, cm
B_{F_0}	auxiliary conversion factor for lap-belt force, kg/cm/sec^2
B_{TR}	backrest translational drive component, cm
C_i	contour drive components, cm
D_i	drive vector for backrest, seat pan, and thigh panels, $i = 1-31$, dimensionless
D_{LB}	drive for lap belt, dimensionless
d_c	critical difference statistic
E_p	aircraft roll energy, J
E_r	aircraft yaw energy, J
e_j, b_j	shaping parameters for distortion of input dynamics, $j = x,y,z,\dot{p},p$
F_0	primary conversion factor for lap-belt force, kg/cm/sec^2
g	acceleration due to gravity, 980.621, cm/sec^2
IBAT	enable/disable switch for backrest attitude drive, dimensionless
IBELT	enable/disable switch for lap-belt drive, dimensionless
IBTR	enable/disable switch for backrest translational drive, dimensionless
IFR	instrument flight rules
IMOT	motion switch; closed for combined operation of g-seat and motion system
IRAC	roll dynamics input mode switch, dimensionless
IROT	enable/disable switch for roll-dynamics input, dimensionless
ISAT	enable/disable switch for seat-pan attitude drive, dimensionless
ISTR	enable/disable switch for seat-pan translational drive, dimensionless
IXC	enable/disable switch for x-acceleration influence on backrest contouring, dimensionless

IYC enable/disable switch for y-acceleration influence on backrest and seat-pan contouring, dimensionless

IZC enable/disable switch for z-acceleration influence on seat-pan contouring, dimensionless

K_{BC} independent gain for backrest contouring, dimensionless

K_{BF} reduction coefficient for gravity component influence on lap-belt drive, dimensionless

K_{BTR} independent gain for backrest translation, sec^2

K_{CPL} gain for seat-pan excursion to lap-belt coupling, $dynes/cm^3$

K_{LB} gain for lap-belt drive, $dynes/cm^2$ kg

K_p gain for roll-rate input, cm sec/rad

$K_{\dot{p}}$ gain for roll acceleration input, cm sec^2/rad

K_{SC} independent gain for seat-pan contouring, dimensionless

K_{SH} coefficient for y-acceleration and roll-dynamics influence sharing for backrest and seat-pan contouring, dimensionless

K_{S_i} drive cell dynamics influence vector, $i = 1-31$, dimensionless

K_{STR} independent gain for seat-pan translation, sec^2

K_{W_i} drive cell subject weight distribution vector, $i = 1-31$, kg^{-1}

K_{XAT} gain for x-acceleration influence on backrest and seat-pan attitude, cm/g

K_{XATB} independent gain for x-acceleration influence on backrest attitude, dimensionless

K_{xC} independent gain for x-acceleration influence on backrest contouring, sec^2

K_x gain for x-acceleration influence on backrest translation, backrest contouring, and thigh-panel splay angle, dimensionless

K_{xTH} independent gain for x-acceleration influence on thigh-panel drive, sec^2/cm

K_{xz} gain for x-acceleration and z-acceleration influence on lap-belt contraction, dimensionless

K_{YAT} gain for y-acceleration influence on backrest and seat-pan attitude, cm/g

K_y gain for y-acceleration influence on backrest contouring, seat-pan contouring, and differential thigh-panel deflection, dimensionless

K_{yC} independent gain for y-acceleration influence on backrest and seat-pan contouring, sec^2

K_{yTH} independent gain for y-acceleration influence on thigh-panel drive, sec^2

K_z gain for z-acceleration influence on seat-pan translation, seat-pan contouring, and thigh-panel deflection, dimensionless

K_{zC} independent gain for z-acceleration influence on backrest and seat-pan contouring, sec^2

K_{zTH} independent gain for z-acceleration influence on thigh-panel drive, sec^2

K_ϕ primary gain for roll-dynamics influence, dimensionless

K_{ϕ_I} independent gain for roll-dynamics influence on thigh-panel excursion, dimensionless

K_{ϕ_M} independent gain for roll-dynamics influence on backrest and seat-pan contouring, sec^2/rad or sec/rad

K_{ϕ_s} independent gain for roll-dynamics influence on seat-pan excursion, dimensionless

L aircraft body-axis rolling moment, N·m

N aircraft body-axis yawing moment, N·m

N_i normalization vector for backrest drive, seat-pan drive, and thigh-panel drive, $i = 1-31$, cm^{-1}

N_{LB} normalization factor for lap-belt drive, cm^2/dyne

P_{LB} desired lap-belt actuator pressure, dynes/cm^2

P_{LBN} neutral pressure for lap-belt drive, dynes/cm^2

p structured roll-rate input, body axes, rad/sec^2

$\dot{p}$ structured roll acceleration input, body axes, rad/sec^2

p_B aircraft body-axes roll rate, rad/sec

$\dot{p}_B$ aircraft roll acceleration in aircraft body axes, rad/sec^2

p_{HF} filtered pilot station roll-rate, body axes, rad/sec

$\dot{p}_{HF}$ filtered pilot station roll acceleration, body axes, rad/sec^2

R_{xA_i} drive cell weighting vector for x-acceleration influence on backrest and seat-pan attitude, $i = 1-25$, dimensionless

R_{x_i} drive cell weighting vector for x-acceleration influence on backrest contouring, $i = 17-25$, dimensionless

R_{yA_i} drive cell weighting vector for y-acceleration influence on backrest and seat-pan attitude, $i = 1-25$, dimensionless

R_{y_i} drive cell weighting vector for y-acceleration influence on backrest and seat-pan contouring, $i = 1-25$, dimensionless

R_{yz} scale factor for roll-dynamics influence on backrest and seat-pan contouring, cm

R_{z_i} drive cell weighting vector for z-acceleration influence on seat-pan contouring, $i = 1-16$, dimensionless

r_B aircraft body-axes yaw rate, rad/sec

S_{TR} seat-pan translational drive component, cm

$\bar{S}$ average seat-pan excursion for lap-belt coupling, cm

S_ϕ seat-pan roll drive component, cm

T_i thigh-panel drive components, $i = 26-31$, cm

T_{s_i} drive cell weighting vector for y-acceleration and roll-dynamics influence on thigh-panel drive, $i = 26-31$, dimensionless

T_{x_i} drive cell weighting vector for x-acceleration influence on thigh-panel drive, $i = 26-31$, cm

$T31$ aircraft direction cosine = $\cos\phi \sin\theta \cos\psi + \sin\phi \sin\psi$

$T33$ aircraft direction cosine = $\cos\phi \cos\theta$

t_e task end time, sec

t_o task start time, sec

VFR visual flight rules

W subject weight, kg

W_a pilot's control wheel activity integral, deg^2

x_{TH} x-acceleration input threshold, cm/sec^2

$\ddot{x}$ structured x-acceleration input, body axes, cm/sec

$\ddot{x}_{HF}$ filtered pilot station x-acceleration, body axes, cm/sec^2

$\ddot{x}_p$ pilot station x-acceleration in aircraft body axes excluding gravity component, cm/sec^2

y_{TH} y-acceleration input threshold, cm/sec^2

$\ddot{y}$ structured y-acceleration input, body axes, cm/sec

$\ddot{y}_{HF}$ filtered pilot station y-acceleration, body axes, cm/sec^2

$\ddot{y}_p$ pilot station y-acceleration in aircraft body axes excluding gravity component, cm/sec^2

z_{TH} z-acceleration input threshold, cm/sec^2

$\ddot{z}$ structured z-acceleration input, body axes, cm/sec

$\ddot{z}_{HF}$ filtered pilot station z-acceleration input, body axes, cm/sec^2

$\ddot{z}_p$ pilot station z-acceleration in aircraft body axes excluding gravity component, cm/sec^2

δ_{A_i} distribution multiplier for backrest and seat-pan attitude drive, i = 1–31, dimensionless

δ_{B_i} distribution multiplier for backrest translational drive, i = 1–31, dimensionless

δ_{C_i} distribution multiplier for backrest and seat-pan contour drive, i = 1–31, dimensionless

δ_{S_i} distribution multiplier for seat-pan translational drive, i = 1–31, dimensionless

δ_{T_i} distribution multiplier for thigh-panel drive, i = 1–31, dimensionless

δ_w pilot's control wheel deflection, deg

δ_{ϕ_i} distribution multiplier for seat-pan roll drive, i = 1–31, dimensionless

ϕ_{CC} contour excursion command due to roll, cm

ϕ_{CI} thigh-panel excursion bias due to roll, cm

ϕ_{CS} seat-pan excursion bias due to roll, cm

THE EFFECTS OF MOTION AND G-SEAT CUES ON PILOT SIMULATOR PERFORMANCE OF THREE PILOTING TASKS

Thomas W. Showalter and Benton L. Parris

Ames Research Center

SUMMARY

Data are presented that show the effects of motion system cues, g-seat cues, and pilot experience on pilot performance during takeoffs with engine failures, during in-flight precision turns, and during landings with wind shear. Eight groups of USAF pilots flew a simulated KC-135 using four different cueing systems. The basic cueing system was a fixed-base type (no-motion cueing) with visual cueing. The other three systems were produced by the presence of either a motion system or a g-seat, or both. Extensive statistical analysis of the data was performed and representative performance means were examined. These data show that the addition of motion system cueing results in significant improvement in pilot performance for all three tasks; however, the use of g-seat cueing, either alone or in conjunction with the motion system, provides little, if any, performance improvement for these tasks and for this aircraft type.

INTRODUCTION

Many modern flight simulators attempt to provide aircraft acceleration cues as well as aircraft visual and auditory cues. Typically, the acceleration cues have been presented by physical motion of the simulator cab. This report is concerned with comparing that mode of acceleration cueing with g-seat cueing.

The g-seat is designed to create the illusion of acceleration by presenting the pilot with those somatic stimuli (i.e., skin pressure, body position) that are thought to be closely associated with the pilot's perception of whole-body acceleration.

The basic development of the g-seat, performed by Kron (ref. 1), resulted in the creation of the g-seat system used for this study. This developmental work by Kron also included the creation of a cueing scheme that was only slightly modified for use in this study.

The present experiment, a joint NASA/USAF effort, was designed as a transfer-of-training study. Both Phase I (training) and Phase II (evaluation of training) of the experiment were conducted at Ames Research Center using the Flight Simulator for Advanced Aircraft (FSAA) to simulate the KC-135A aircraft.

This report considers the effects of the motion system and g-seat on pilot performance during the Phase I portion of the experiment. The analysis of the Phase II portion has been performed by a

USAF engineering group (ASD/ENC) at Wright-Patterson Air Force Base, Ohio, and is reported in a separate publication (ref. 2).

The g-seat and motion systems used for this study, although conceptualized as representative of the g-seat and motion system concepts, are still specific pieces of hardware, with pilot performance effects specific to the design of each. As designs change, pilot performance may also change. For that reason, the conclusions presented herein should be related only to g-seat and motion systems of comparable design and only to similar tasks, pilots, and aircraft.

EXPERIMENTAL DESIGN

The experiment was designed to examine the effects of different acceleration cueing techniques on pilot-simulator performance of three tasks: takeoff with engine failure, precision turns, and landing with wind shear.

The structure, an independent groups design, consisted of eight groups of six pilots each. The groups were defined by the permutation of three independent variables: (1) motion system – present (M) or absent (F); (2) g-seat – present (GS) or absent (NS); and (3) pilot type – high time (H) or low time (L).

The eight groups were as follows:

Conditions	Abbreviation
G-seat X motion X high time	GSMH
G-seat X motion X low time	GSML
G-seat X no motion X high time	GSFH
G-seat X no motion X low time	GSFL
No g-seat X motion X high time	NSMH
No g-seat X motion X low time	NSML
No g-seat X no motion X high time	NSFH
No g-seat X no motion X low time	NSFL

The advantage of this type of experimental design is that group differences can isolate several effects: they can highlight the differences and the similarities in the information-producing capabilities of g-seat and motion systems; they can reveal the relative abilities of high-time and low-time pilots; and across tasks, they can serve to determine whether the effects of g-seat cueing, motion cueing, and pilot type are task-dependent.

METHOD

Apparatus

The six-degree-of-freedom Flight Simulator for Advanced Aircraft (FSAA, fig. 1) was used for this study. The different training systems were created by restricting or augmenting the FSAA in some well-defined manner.

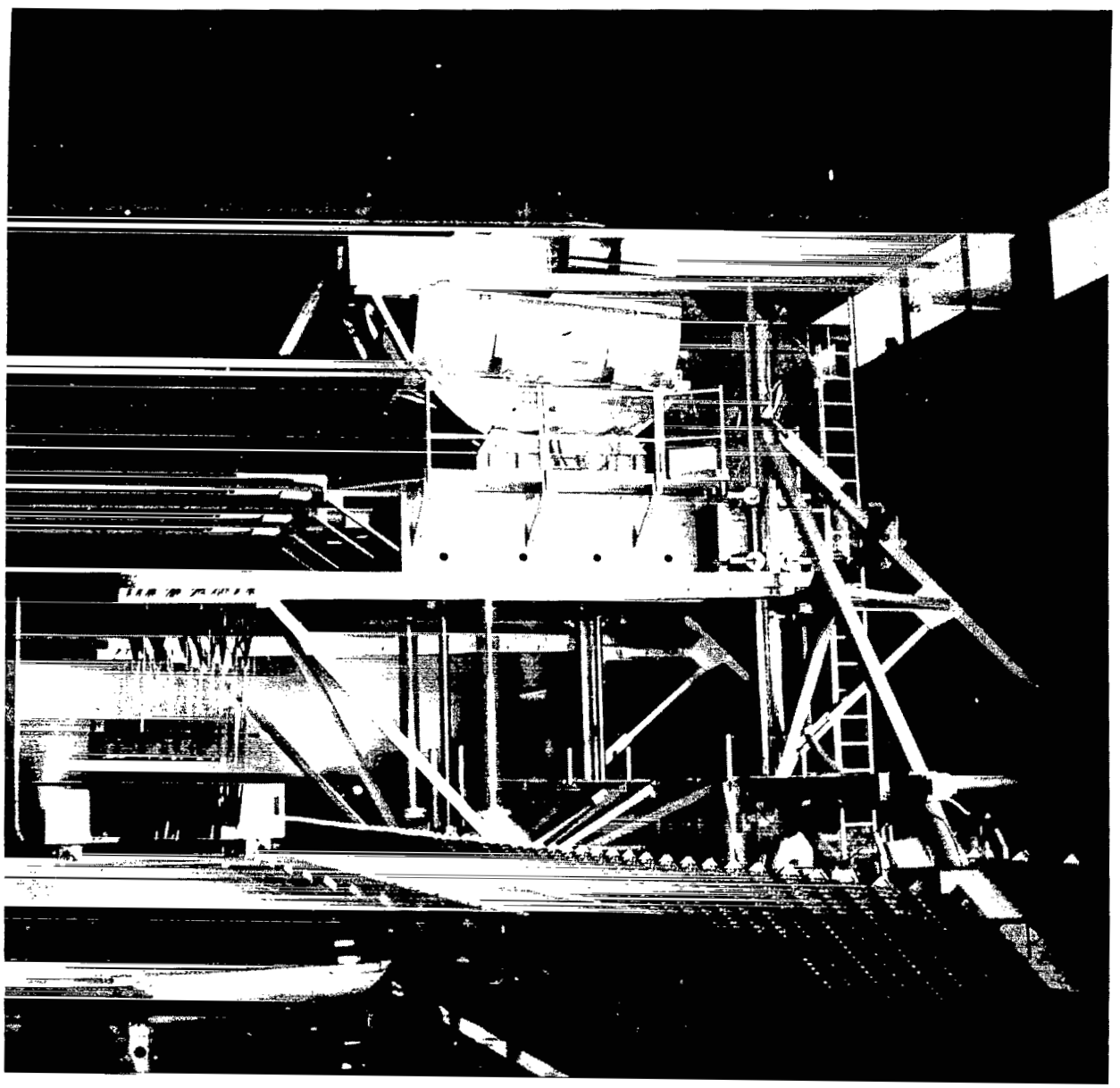

Figure 1.— The six-degree-of-freedom Flight Simulator for Advanced Aircraft (FSAA) at Ames Research Center.

The simulator visual system, present in all training systems, consisted of a gantry-mounted color television camera which moved relative to a fixed model board as directed by the simulation computer. The visual scene was presented to the pilot by a cathode-ray-tube display affixed to a set of collimation optics situated in the forward cockpit window. The viewing angles at the pilot's eye were 36° vertically and 45° horizontally.

The motion system, as used during Phase I (training), was restricted by the drive program in the simulation computer (ref. 3) to simulate a synergistic six-degree-of-freedom motion system. For that system, the normal independent axis operation of the FSAA motion was restricted so that not only were the travel limits reduced, but dynamic limiting was performed contingent on simulator position.

The g-seat, shown in figure 2, was mounted in the FSAA cab at the pilot's position; it consisted of 29 pneumatic cells in the seat back, pan, and thigh panels. In addition, a pneumatically controlled lap-belt force mechanism was provided. The seat cells and lap-belt force mechanism were all separately controlled by an array of 30 servovalves, rack-mounted on the top of the FSAA cab. The servovalves were driven by commands from the simulation computer.

In general, the cueing scheme implemented in the g-seat drive program incorporated a "surface pressure" philosophy that required the seat cells to inflate or deflate such that the skin pressure sensed by the pilot was in the same direction as the aircraft acceleration vector. For example, during a pull-up maneuver, seat-pan cells inflated to increase the overall pressure on the pilot's buttocks. However, contouring was also implemented to relieve some of the inherent conflict between pressure and position information. For the example just cited, although the overall seat-pan pressure was increased, the center rows of the seat pan were inflated to a much lesser degree, an attempt to create the illusion of sinking into the seat.

The "surface pressure" philosophy was used to cue accelerations in the longitudinal (x) and vertical (z) axes at the pilot's station and to cue aircraft roll rate. Contouring was used in the z axis and roll only. The lateral (y) axis accelerations at the pilot's station were cued by an attitude drive scheme whereby the seat-pan and backrest planes were tilted in opposition to the direction of the y-axis acceleration; that is, left tilt for rightward acceleration.

The lap-belt mechanism was driven to augment the cueing in the x-z plane. For example, the lap-belt force was reduced for a pull-up maneuver and increased for a push-over maneuver.

Further details of the g-seat hardware and drive scheme used for this study are presented in appendix A and in reference 4.

The FSAA cab was configured with representative flight instruments and controls (fig. 3), including wheel, column, and rudder pedals with programmed force-feel characteristics designed to resemble those of the KC-135A aircraft.

The sound simulator provided auditory cues to the pilot through stereo speakers located at the right and left rear of the simulator cab. Sound generation was based on real-time information from the simulation computer, including thrust level for each of the four engines, airspeed, and landing gear discrete event information. The sound system simulated turbojet engine sound for each of the four engines which, in the engine failure event, provided the pilot with an engine spool-down cue. Additional auditory cueing included airspeed sound, gear up/down thumps, and weight-on-wheels thump.

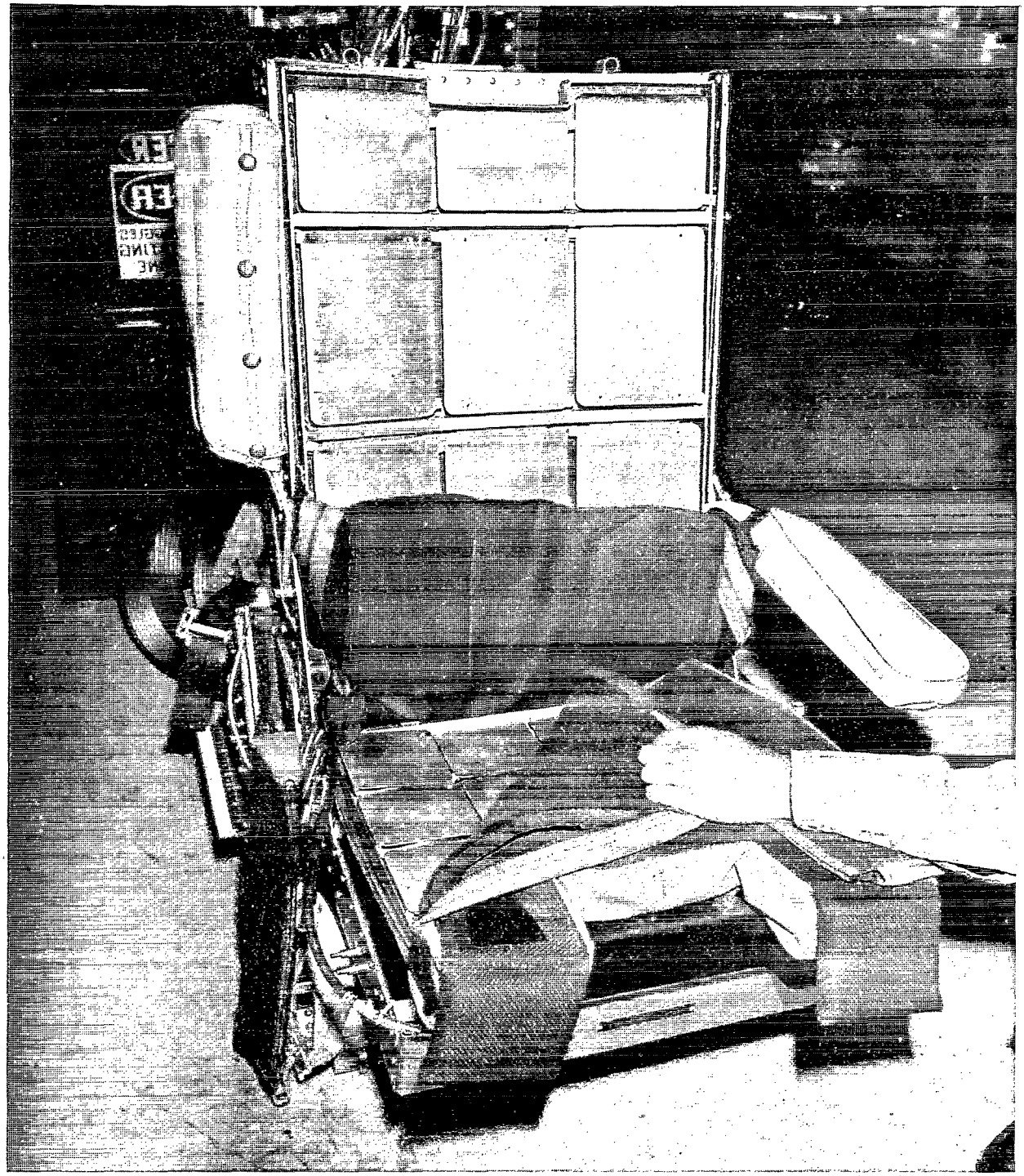

Figure 2.– The g-seat after modification to transport-type substructure.

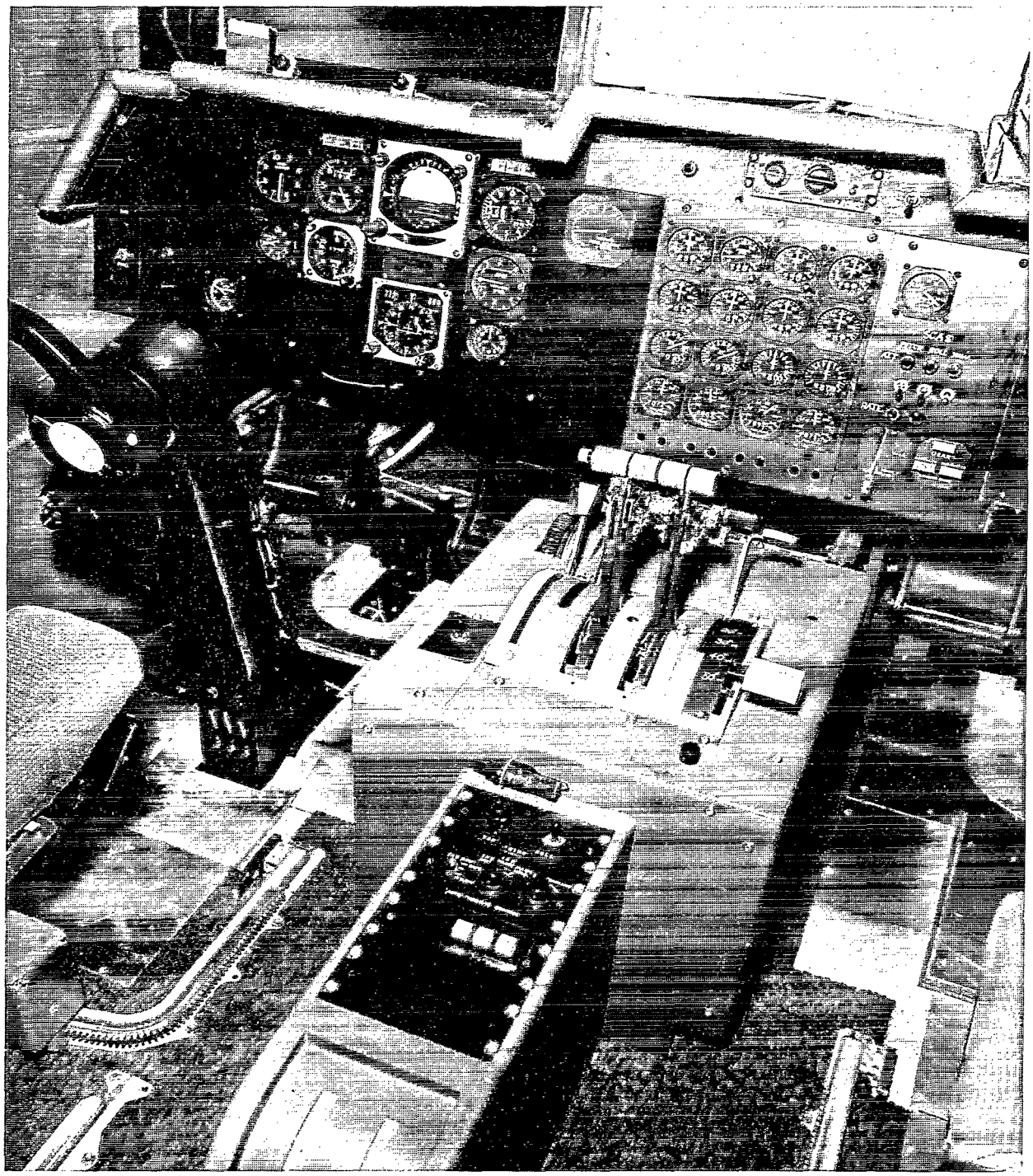

Figure 3.– The FSAA cab layout for the KC-135A simulation.

The aircraft model and associated equations of motion, implemented in the simulation computer, were the same as those used in a previous simulation experiment with the KC-135A (ref. 5).

Subjects

Forty-eight U.S. Air Force pilots from the Strategic Air Command (SAC) were used as test subjects. Each was a KC-135 aircraft commander currently qualified in the aircraft. The subjects were divided into two subgroups for testing. One group consisted of 24 pilots who had more than 500 hr of flying time (high time) and the other group contained 24 pilots who had less than 500 hr (low time). The high-time group averaged 1484.2 hr of flight time and the low-time group averaged 270.3 hr.

Procedure

Prior to Phase I of this experiment, the pilots became familiar with the FSAA and the g-seat by flying a series of normal takeoffs, normal landings, and turns. Thereafter, every pilot, whether high time or low time, was randomly assigned to one of four training systems (e.g., g-seat with motion, GSM) that he was to use throughout his Phase I session.

In Phase I, every pilot performed the following three tasks: (1) takeoff with an outboard engine failure, (2) precision turns, and (3) approach and landing with wind shear. The session of each pilot was considered complete when his performance no longer showed noticeable improvement on any task.

Task 1, takeoff with an outboard engine failure, was an emergency-procedure maneuver that required the pilot to respond quickly with appropriate rudder and wheel inputs to control the simultaneous yawing and rolling caused by the engine failure.

The takeoff engine failure conditions, which were standardized across subjects, were varied randomly on a trial-to-trial basis within subjects. The sequence shown in appendix B was created by randomly varying the altitude of the engine failure and the engine failed (i.e., left or right outboard). All engine failures occurred after the pilot had committed to rotate and climb out. A trial ended when the pilot had successfully executed the climb-out by passing through an altitude of 304.8 m (1000 ft). All trials occurred under full visual flight rules (VFR conditions).

Task 2, the precision turns, required the pilot to maintain precise control of bank angle, airspeed, rate of climb, and heading. Each trial consisted of, in sequence, one ascending 180° turn, a short period of straight and level flight, and a descending 180° turn. Each turn required an altitude change of 213.4 m (700 ft), which was to be accomplished at a rate of 304.8 m/min (1000 ft/min), a constant airspeed of 277.8 km/hr (150 knots), and at a 30° bank angle. The direction (right or left) of each turn was varied randomly within every subject's sequence, but across subjects all sequences were the same (see appendix B). All trials were conducted under instrument flight rules (IFR conditions).

The difficulty of Task 3, landing with wind shear, was varied from trial-to-trial by varying the wind shear conditions. The difficult wind shear conditions induced a severe Dutch roll (simultaneous rolling and yawing of the aircraft), requiring the pilot to quickly assess the situation and make

the appropriate rudder pedal and wheel inputs. The moderate wind shear conditions forced the aircraft off the intended approach path, requiring the pilot to adjust the rate of descent and heading in order to return to the approach path. The sequence of wind shear conditions varied randomly within subjects, but was constant across subjects. A light amount of turbulence was also present during the wind shear trials. The sequence of wind shear conditions and details of the wind and turbulence model used are presented in appendix B.

With the exception of wind shear conditions, all approach conditions were held constant and were conducted under VFR conditions. The subjects were required to intercept the glide slope (3°) and localizer at an altitude of 304.8 m (1000 ft) and to attempt to remain on glide slope and localizer until flare and touchdown. Each trial ended just after touchdown.

Scoring

Numerous performance parameters were recorded for each task during Phase I and Phase II of this experiment. As mentioned in the Introduction, the analysis of the Phase II data was performed by a USAF engineering group (ref. 2) and was concerned with the transfer of training effects. This report, however, concerns an analysis of the Phase I data only and examines the effects of the various cueing systems on pilot performance. It was not known, prior to the experiment, which performance parameters could be used to best describe and interpret pilot performance during Phase I; therefore, post-experimentation methods were used.

Factor analysis programs (ref. 6) were used to organize the data and select performance measures for each task. This analysis, which was based on performance data averaged across trials for each subject, examined the covariance between parameter means and subjects. Performance parameters that covaried simultaneously indicated that these parameters changed value in like ways under like circumstances and were, therefore, grouped to form a common dimension or factor.

For each task, the factor analysis program was used to compute 10 factors. The factors that accounted for most of the variance across subjects and that, by virtue of the performance parameters in their association, had obvious relevance to the task in question, were chosen as the most predictive factors. The performance parameter that correlated most highly with a predictive factor was selected as a performance measure for that task.

The performance measures chosen (see Results) are defined as follows:

$$E_p = \int_{t_o}^{t_e} |L \cdot p_B| dt\,, \quad \text{J}$$

$$E_r = \int_{t_o}^{t_e} |N \cdot r_B| dt\,, \quad \text{J}$$

$$W_a = \int_{t_o}^{t_e} \delta_w{}^2 \cdot dt/(t_e - t_o)\,, \quad \text{deg}^2$$

The Task 1 performance measure, E_r, is the integral of aircraft yaw power or the energy in yaw. The calculation of this integral began at the time of engine failure (t_o) and ended (t_e) when the aircraft passed the altitude of 304.8 m (1000 ft) above field elevation. A low value of E_r indicates that very little yaw energy was generated after the engine failure, which means that the pilot responded quickly to the engine failure and rapidly regained control of the aircraft. A high value of E_r indicates the opposite. The "Dutch roll," which normally accompanies an outboard engine failure for this aircraft, involves both roll and yaw motion. However, the amount of yaw activity was determined to be a more sensitive indicator than the roll activity for measurement of pilot performance for this task.

The Task 2 performance measure, E_p, is the integral of aircraft roll power or the energy in roll. The values of E_p for Task 2 are the sum of two integrals, one for each of the ascending and descending turns. The calculation of these integrals began at the start of a turn (t_o) and ended when the aircraft was rolled straight and level (t_e). Straight and level was defined as aircraft roll angle maintained below 5° for at least 3 sec. The E_p measure is sensitive to bank angle changes and as such is an indicator of how well the pilot maintained control of the aircraft in precision turns. High values of E_p indicate poor performance, and low values indicate good performance.

The calculation of the E_p and W_a integrals for Task 3 began when the glide slope was intercepted at 304.8 m (1000 ft) altitude (t_o) and ended at touchdown (t_e). Again, high values of E_p indicate poor performance and low values indicate the opposite.

The W_a measure is a time average of what is normally termed wheel control power and is sensitive to changes in levels of activity that the pilot devotes to roll control.

After selecting the performance measures for each task, analysis-of-variance programs (ref. 7) were used to determine which interactions of the experimental variables were statistically significant. The experimental variables were: synergistic motion (presence/absence), g-seat (presence/absence), pilot type (high-time or low-time), and trials. The interactions selected by this process always involved at least two experimental variables and thereby reduced the possibility of any simple main-effects data interpretations. Statistical significance in this respect meant that the intergroup differences for the interaction in question were so great as to preclude their occurrence by chance. To determine which intergroup differences for any given interaction were significant (occurred for reasons other than chance), the critical difference (d_c) criterion (ref. 8) was applied. Intergroup differences less than the critical difference are chance variations and those in excess are not. The critical difference values are presented with the data in figures 4–9.

RESULTS

The results of the factor analysis are presented in table 1. Only one predictive factor each emerged for Task 1 and Task 2 and, therefore, pilot performance differences for those tasks are described by only one performance measure. Two orthogonal predictive factors emerged for Task 3 resulting in two performance measures. The results of subsequent analyses of the selected measures are presented below according to task.

TABLE 1.– PERFORMANCE MEASURES

Task	Variance associated with principal factor	Principal measure	Correlation of measure with factor
1. Takeoff with engine failure	Factor 1 38.0%	Energy in yaw, E_r	0.962
2. Precision turns	Factor 1 36.7%	Energy in roll, E_p	0.966
3. Landing with wind shear	Factor 1 28.8%	Wheel activity, W_a	0.906
	Factor 2 17.4%	Energy in roll, E_p	0.960

Task 1: Takeoff with Engine Failure

The motion X g-seat interaction showed significant group differences with $\alpha \leqslant 0.05$. The E_r data for this interaction were averaged across trials and pilot-type variables. These means are presented in figure 4. The critical mean difference statistic (d_C) shows that the mean for the no-motion/no-g-seat condition (NSF) is significantly greater than the means for the other three conditions, and that the mean for the no-motion/g-seat condition (GSF) is significantly greater than the mean for the motion/no-g-seat (NSM) condition.

The motion X pilot type X trials interaction also showed significant group differences with $\alpha \leqslant 0.05$. This interaction is shown in figure 5, where the E_r data for each pilot-type/motion condition combination, averaged across g-seat conditions, is plotted versus trials. For Trials 1–6, the performances varied a great deal as a function of pilot type and in such a fashion that it is difficult to cite a simple effect. Neither high-time nor low-time pilots were consistently better or worse than the other. However, during that segment of trials, the motion-cued performances displayed much less variance than did the nonmotion-cued performances.

In general, as shown in table 2, the motion variable, accounting for 58.3% of the variance, had a more profound effect on performance than did g-seat, pilot type, or trials variables.

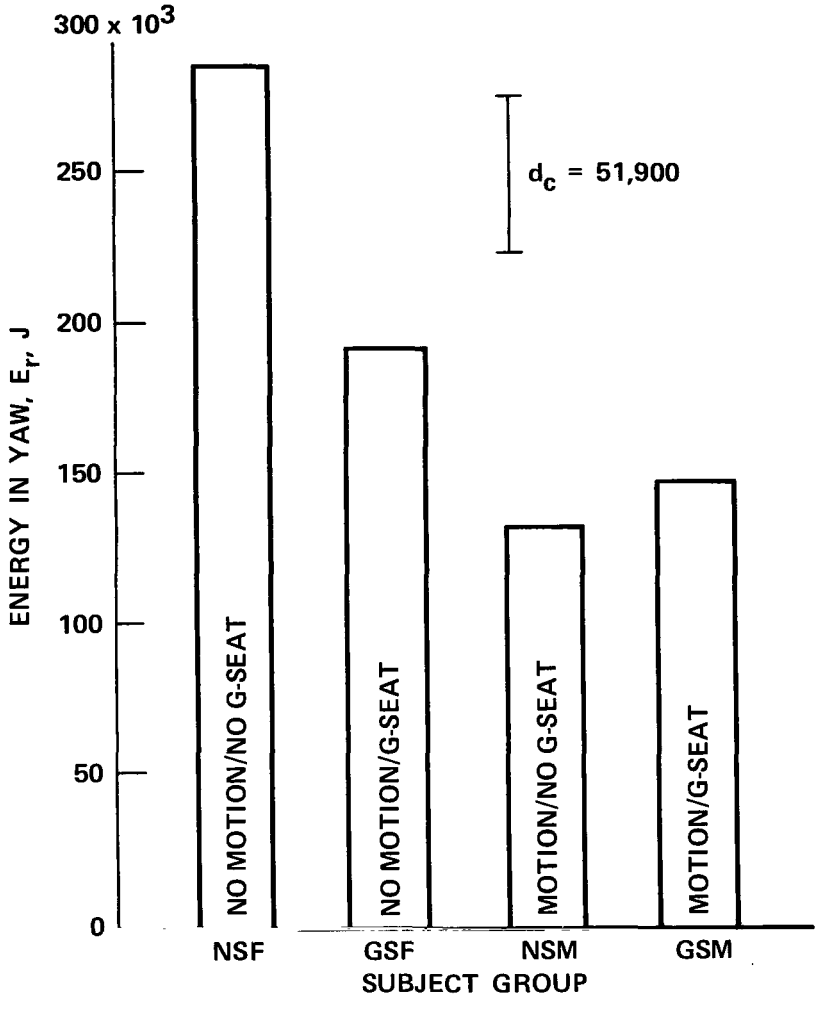

Figure 4.– Motion X g-seat interaction for Task 1 in terms of mean E_r performance.

Task 2: Precision Turns

For this task, the motion X g-seat X pilot type interaction showed significant group differences with $\alpha \leqslant 0.06$. The E_p data for this interaction were averaged across trials and are presented in figure 6. The no-motion/g-seat/low-time condition (GSFL) mean is significantly greater than the means for either the no-motion/g-seat/high-time (GSFH) or the motion/no-seat/high-time (NSMH) conditions. As shown in table 2, the pilot type variable accounted for the most nonerror variance. It should be noted that only for this task was the error variance higher than the variance accounted for by any of the experimental variables.

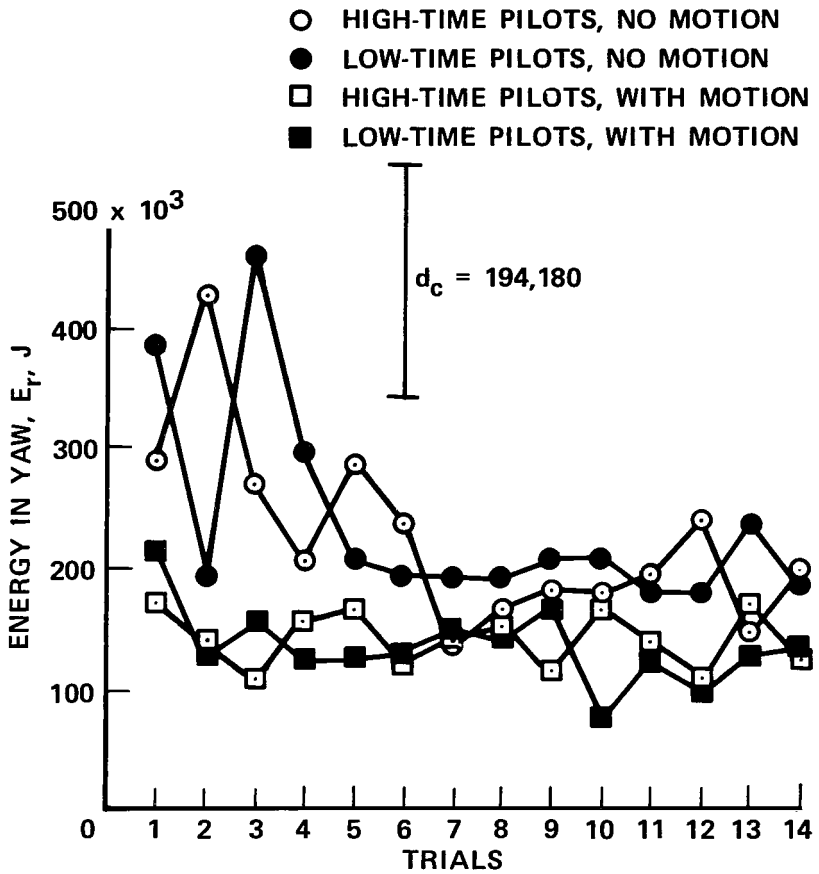

Figure 5.– Motion X pilot type X trials interaction for Task 1 in terms of mean E_r performance.

TABLE 2.– DISTRIBUTION OF PERFORMANCE VARIANCE

Experimental variables	Task 1: takeoff with engine failure	Task 2: precision turns	Task 3: landing with wind shear	
	E_r, %	E_p, %	W_a, %	E_p, %
G-seat	8.9	1.6	0.2	1.2
Motion	58.3	11.8	58.7	9.7
Pilot type	.1	25.7	3.1	4.6
Trials	2.5	1.7	13.3	47.6
Interactions and error terms	30.2	59.2	24.7	36.9

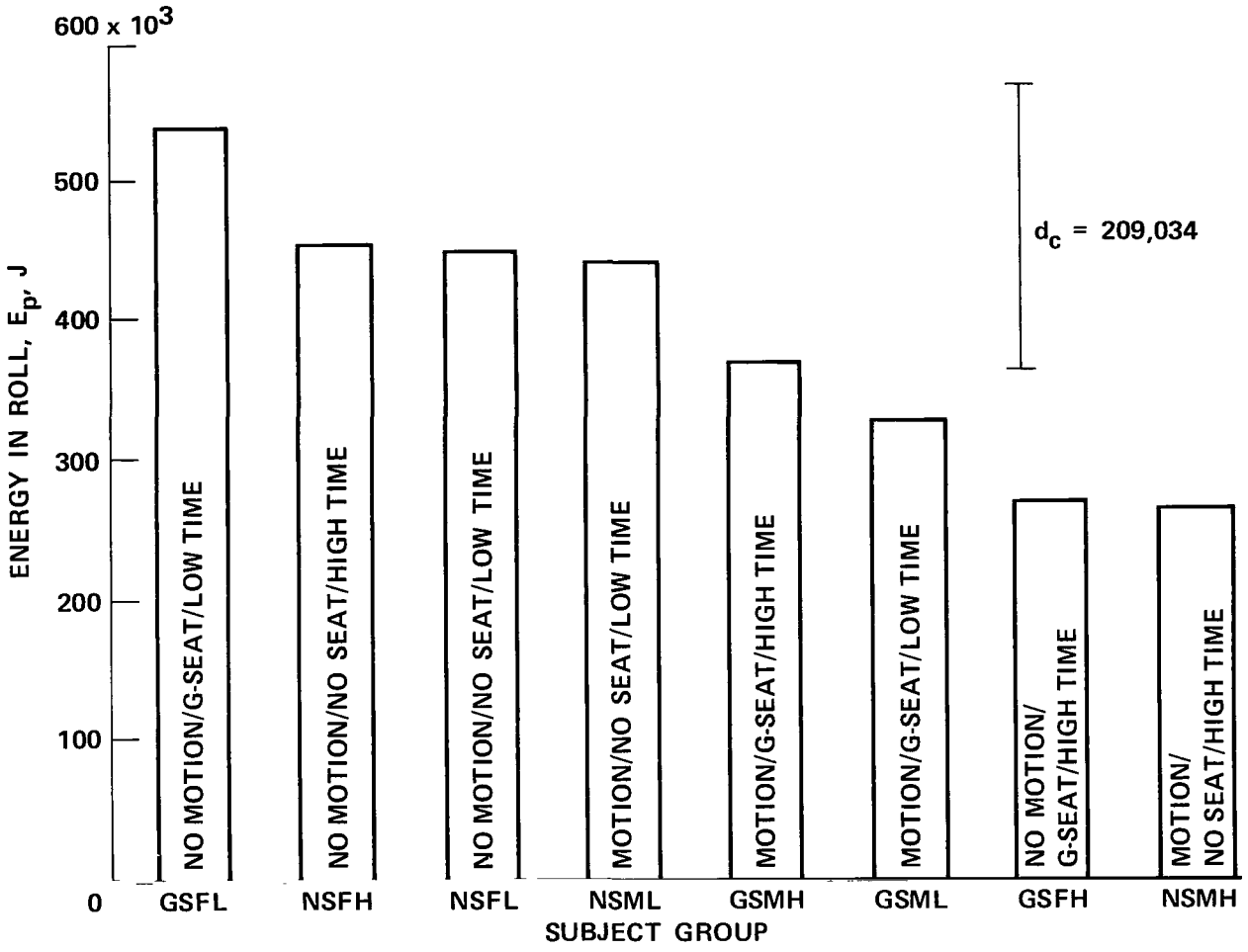

Figure 6.– Motion X g-seat X pilot-type interaction for Task 2 in terms of *Ep* mean performance.

Task 3: Landing with Wind Shear

Analysis of the W_a data for this task revealed a motion X g-seat X wind shear interaction with group differences that were significant with $\alpha \leqslant 0.06$. Most of the variance (58.7%) for this measure was accounted for by the motion variable (table 2). The W_a data were averaged across pilot types and are presented in figure 7. According to the critical-difference statistic, the significant mean differences occurred for wind shears 1–4, 6, 7, and 10. For wind shears 1–4 the means for both of the no-motion conditions (i.e., with or without g-seat) were significantly lower than those for their respective motion conditions. For wind shears 6, 7, and 10, however, only the means for the no-motion/g-seat condition were significantly lower than those for the respective motion condition.

Analysis of the E_p data for Task 3 revealed two interactions with significant ($\alpha \leqslant 0.5$) group differences. For the pilot type X wind shear interaction (fig. 8), the E_p data were averaged across motion and g-seat variables. The only significant mean difference for this interaction occurred for wind shear 2, where the mean for low-time pilots was significantly higher than that for high-time

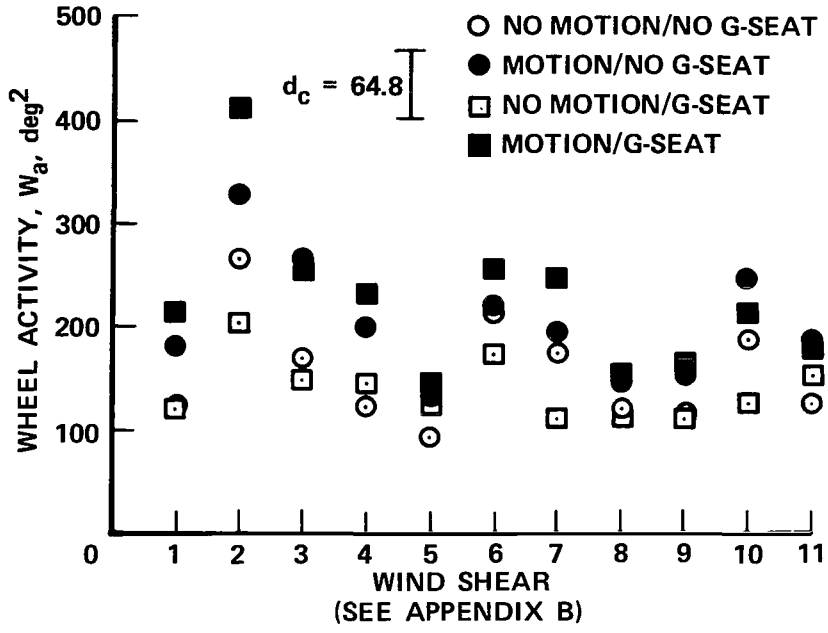

Figure 7.– Motion X g-seat X wind shear interaction for Task 3 in terms of W_a mean performance.

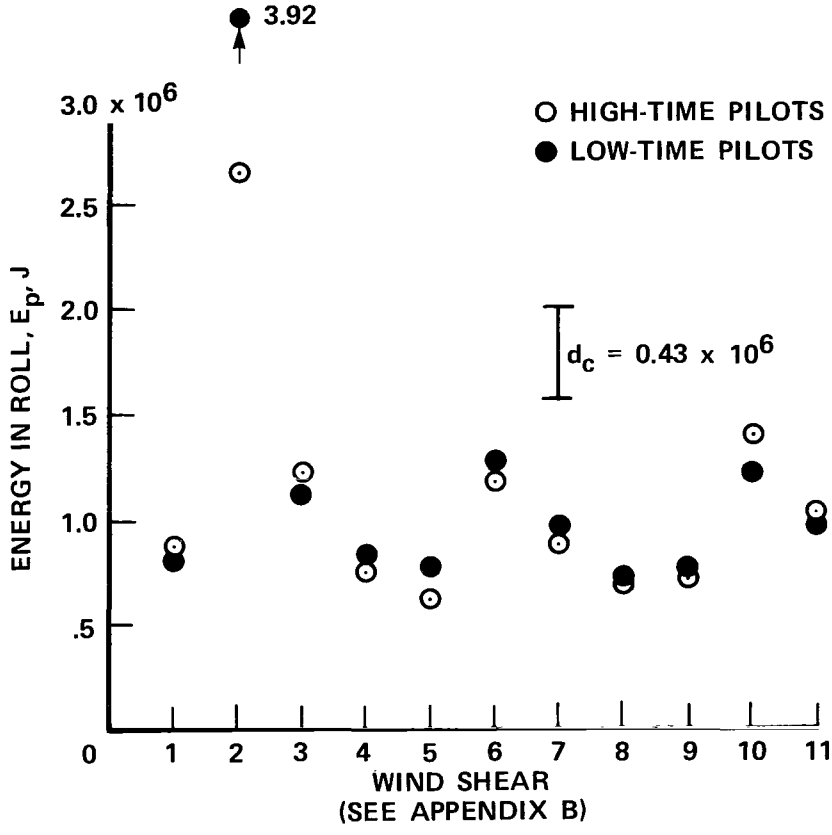

Figure 8.– Pilot type X wind shear interaction for Task 3 in terms of E_p mean performance.

pilots. For the motion X g-seat X wind shear interaction (fig. 9), the E_p data were averaged across the pilot type variable. Significant mean differences for these data occurred for wind shears 2, 6, and 10. For wind shear 2, the mean for the no-motion/no-g-seat condition was significantly higher than those for the other three conditions. For wind shear 6, the mean for the no-motion/g-seat condition was significantly higher than that for the motion/no-g-seat condition. A similar situation occurred for wind shear 10, in which the mean for the no-motion/g-seat condition was significantly higher than the means for either of the conditions with motion-cueing present. It should be noted that, for this task, most of the variance (47.6%) in the E_p data was accounted for by the wind shear (trials) variable (table 2).

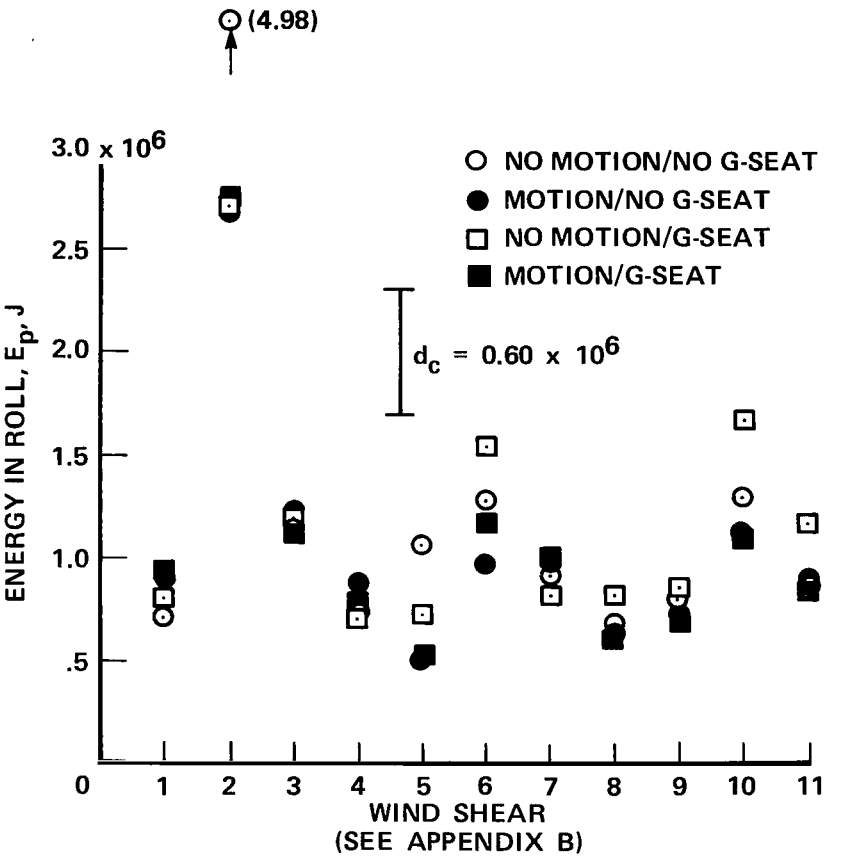

Figure 9.– Motion X g-seat X wind shear interaction for Task 3 in terms of E_p mean performance.

DISCUSSION

The discussion of the results of this study is organized into four subsections. The first three are discussions of the results for Tasks 1, 2, and 3, and the fourth is a comparison of g-seat and motion cueing effects for all three tasks.

Task 1: Takeoff with Engine Failure

The outboard engine failure encountered in Task 1 causes the aircraft to begin to Dutch roll. The Dutch roll, which is a simultaneous yawing and rolling, can be controlled and corrected if the pilot responds quickly with the appropriate rudder input followed by coordinating wheel movements. To accomplish this, the pilot needs timely information that will quickly convey to him the direction and rate of the yaw and roll motions created.

As shown in figure 4, the motion/no-g-seat condition (NSM) produced the best E_r mean score. When compared to the no-motion/no-g-seat condition (NSF) mean, it is obvious that the aircraft simulator motion cues aided the pilots immensely. It is also obvious that the simulator motion cues were more useful to the pilots than were the g-seat cues, as the comparison of the GSF mean with the NSM mean indicates. However, as shown in figure 5, the effects of the motion variable on the E_r data are more complicated than figure 4 suggests.

The results show three basic trends. One is that the performance of the engine-failure task in a no-motion environment affected high-time and low-time pilots differently. It is apparent that performance problems occurred on trials 1–4 and that such problems related to high-time and low-time group differences. The differences were not just simple differences in skill level, however, for simple skill differences would have fostered a consistency in group differences (e.g., one group consistently performing better than the other) that did not occur. These differences might be attributed to the adaptation techniques that each group employed to cope with performing the task in the no-motion environment.

The second trend is that, although both high-time and low-time groups of nonmotion-cued pilots differed initially, both groups made the necessary adjustments in approximately the same number of trials. The reason for this trend is probably quite complex and impossible to ascertain given only the existing data.

The third and perhaps most important trend is that the nonmotion-cued groups, although performing worse initially, eventually improved and reached performance levels comparable to those of the motion-cued groups who performed consistently well throughout the testing. This same trend was exhibited in the results of a previous study involving engine failures in the simulated KC-135 aircraft (ref. 5). The improvement of the nonmotion-cued pilots indicates that they eventually found a means of more effectively utilizing the information presented by the simulator visual scene, instruments, and sound system. This was, however, a difficult process initially. The implication is that pilots, who have primarily aircraft flight experience with very little simulator experience, entered the test conditioned to perceiving and using both visual and vestibular cues to perform an engine-out emergency maneuver. Using a nonmotion simulator required them to alter certain techniques and to find methods of adapting to the visual-only environment. Once the adaptation process was complete, the nonmotion-cued performance was comparable to the motion-cued performance.

It is not known whether using a visual-only environment is more taxing or not. If it were, consistent performance differences could be sustained if the engine-failure task were made more difficult.

It is noteworthy, also, that the presence or absence of g-seat cueing did not significantly affect engine-out performance data. The g-seat variable accounted for a low percentage of the nonerror

variance and there were no significant g-seat X trials interactions. Apparently, g-seat cues are not essential to performance of this task.

Task 2: Precision Turns

Task 2 was designed to require a precision maneuver with no emergency procedures involved; it required the pilots to maintain precise control of bank angle, airspeed, rate of climb, and heading. Because this task was performed under IFR conditions (no outside visual cues), the pilots had to rely heavily on instruments and on backup information from either the motion cue or g-seat (when available), or both.

As shown in table 2, the error variance accounted for the largest portion of the variance in the E_p data for this task. The large amount of error variance, which is composed largely of intersubject differences (irrespective of high-time or low-time rating), suggests that individual performance varied greatly. This, coupled with the fact that the pilot-type variable accounted for most of the nonerror variance (table 2), indicates that performance for this task was primarily a function of pilot ability.

The significant difference between the no-motion/g-seat/low-time (GSFL) group mean and the no-motion/g-seat/high-time (GSFH) group mean (fig. 6) shows that high-time pilots were able to effectively use g-seat cues, whereas low-time pilots in the same cueing system were not. This performance difference suggests that pilots with more flight experience may have different abilities regarding the perception of tactile cues. Increased flight experience may condition a pilot to be more aware of relevant and useful cues.

The occurrence of the significant difference between the no-motion/g-seat/low-time and the motion/no-seat/high-time means (fig. 6) might also be attributed to the pilot-type difference; however, due to the covariance of g-seat, motion, and pilot-type variables, it is difficult to assert which changes in conditions caused the performance difference.

Given the small group size (six subjects per group), it is possible that the "power" of the analysis of variance was low. "Power" is the probability of correctly rejecting the hypothesis that all groups are equal. Even though the analysis of variance showed that the interaction (fig. 6) was significant, when power is low it is less likely that actual group differences have been detected. Therefore, it is risky to rely heavily on the significant group differences shown in figure 6.

Task 3: Landing with Wind Shear

This task was a VFR approach with a wind shear and light turbulence. Some of the wind shear conditions involved large shifts in wind direction and velocity that induced severe Dutch roll of the aircraft. These conditions were quite difficult for the pilots to handle. As with the Dutch roll induced by engine failure, for this task the pilot had to quickly detect changes in the direction and rate of the aircraft roll and yaw and respond with appropriate rudder and wheel inputs.

The W_a and E_p performance measures for this task were functionally dependent on pilot wheel inputs and aircraft roll activity, respectively. The factor analysis showed low correlation of these

two measures across motion, g-seat, and pilot-type variables (orthogonality of factors). This would imply that pilot wheel inputs had little effect on roll activity. However, the factor analysis technique did not examine the within-subject variance across trials, so trial-by-trial correlations between W_a and E_p were not calculated. A comparison of the W_a data (fig. 7) with the E_p data (fig. 9) shows that high values of W_a tended to produce low values of E_p (good performance), and vice versa. Results of a previous study (ref. 5) showed a similar relationship. In that study, however, the performance was degraded if control activity was too high. These trends are obviously related to the phenomena of under-control and over-control of the aircraft.

Two additional clarifications should be made regarding the relationship of W_a and E_p. The first is that these are integral measures and as such are not accurate metrics for moment-by-moment changes. For example, a pilot executing high-frequency, moderate-amplitude wheel inputs could generate the same W_a score as a pilot executing very low-frequency, low-amplitude inputs. The former control technique would have markedly different effects on aircraft roll than the latter. The second clarification is that the wind shear and turbulence, encountered for this task may have obscured the relationship between W_a and E_p. These external disturbances affect roll activity directly and can, in severe conditions, neutralize the wheel input.

The W_a data presented in figure 7 indicate that the presence or absence of motion cues caused a corresponding increase or decrease, respectively, in wheel activity, especially for the more difficult wind shears. This relationship suggests that the addition of motion cues stimulated the pilot frequently, causing him to increase his level of wheel activity. The lack of significant differences in W_a between g-seat and no-g-seat groups (fig. 7) and the low amount of variance (0.2%) accounted for by the g-seat variable (table 2) indicate that the g-seat had very little effect on the pilots wheel activity. If one considers the W_a score to be an accurate indicator of the nature of the pilot/control system interaction, then it could be said that motion cueing greatly affected the pilot's control decision process for this task, and that g-seat cueing seemingly did not.

In figure 8, it is shown that low-time pilots performed significantly poorer for wind shear 2, one of the difficult wind shears, than did the high-time pilots. The absence of significant differences between high-time and low-time pilots on other difficult wind shears, such as 6 and 10, suggests that many low-time pilots eventually adapted to the wind shear task and performed comparably to high-time pilots.

As shown by the E_p data presented in figure 9, the significant motion X g-seat X wind shear interaction occurred under the most difficult wind shear conditions (2, 6, and 10). In every case of significance, the motion/no-g-seat performance was better (lower mean) than that for one of the no-motion conditions. The no-motion/g-seat condition initially produced comparable performance (wind shear 2), but eventually worsened performance (wind shears 6 and 10) in comparison to the motion/no-g-seat condition. These results show that increased exposure to difficult wind shear conditions caused pilots to find no-motion/g-seat cues less usable and eventually obstructionistic, whereas such exposure caused pilots to find motion/no-g-seat cues continually useful.

The consistently superior performance of motion/no-g-seat-cued pilots and the decline of no-motion/g-seat-cued pilots for this task is due to differences in the information value of g-seat and motion system roll and yaw stimuli. Motion system roll and yaw stimuli seemed to maintain a high information value, whereas g-seat stimuli did not.

Another study, which used the same g-seat (ref. 9), dealt specifically with the ability of the g-seat stimuli to cue roll or create the roll illusion. In that study, g-seat stimuli failed to create a suitable roll cue for four of five pilots. They described g-seat roll stimuli as highly stylized and ambiguous. Only by placing special emphasis on perceiving the g-seat roll stimuli were these pilots able to detect aircraft roll rate and direction. It is conceivable that Task 3, being so demanding, did not allow pilots the opportunity to place special emphasis on perceiving and using g-seat roll or yaw stimuli. Had a pilot placed special emphasis on g-seat stimuli, the extra effort required might have caused other aspects of his piloting ability to decline. The real issue is that accurately interpreting an ambiguous cue is a relatively time-consuming task, if not a decidedly risky one. Inferring aircraft roll and yaw rates and directions from g-seat stimuli is definitely a more time-consuming and error-prone process than doing so from motion system stimuli.

Comparison of g-Seat and Motion System Effects

In all three tasks, the presence of motion system cueing consistently improved performance in some manner. The motion variable consistently accounted for large portions of the nonerror variance across tasks (table 2), always accounting for far more variance than the g-seat factor. When compared to the motion, pilot type, or trials variables, the g-seat factor accounted for the least variance on three of the four performance parameters (table 2) and ranked third in effect on the fourth parameter (E_r, Task 1). The presence or absence of g-seat cueing apparently had relatively little overall effect on pilot performance across tasks.

On those specific occasions when the presence of g-seat cueing caused significant performance differences, the effects varied. There were three effects: a decline in performance (Task 3), an ambivalent performance effect (Task 2), or a modest performance improvement (Task 1).

The difference between the value of g-seat versus the value of motion cueing are apparent, especially on the difficult tasks that require the pilot to perceive and effectively use high-frequency roll and yaw cues (e.g., Tasks 1 and 3). On tasks of that sort, motion cueing promoted significantly better performance than g-seat cueing.

It could be that these pilot-performance differences were caused by the limited frequency response characteristics of the g-seat used in this study (ref. 4). This g-seat, when compared to the motion system (ref. 10), has noticeably more phase lag and poorer amplitude response at frequencies above 6 rad/sec. At the higher frequencies, the g-seat provides the pilot with out-dated information, which may cause or contribute to the g-seat pilot performance problems.

The frequency response of the g-seat, although having some effect on the information value of g-seat cues, is not the essence of what is meant by "information." For example, g-seat roll cues, whether from a rapid or slow roll, must easily induce the roll illusion and be of such a nature that the pilot can utilize those cues in the control decision process. Unless the basic mechanical design of the g-seat is capable of easily evoking the proper sensations and inhibiting the unwanted ones, increasing the bandwidth of the g-seat system will not significantly improve g-seat roll or yaw cueing.

A nonoptimum g-seat drive logic could also have caused or contributed to the g-seat performance problems. Given more research and development, g-seat roll and yaw cues could possibly be made comparable in quality to motion system roll and yaw cues. However, after one such

development effort (ref 9) g-seat roll cues were evaluated as ambiguous and unacceptable by four of five pilots. As discussed at length in reference 9, cueing aircraft roll or yaw with g-seats of this design or of similar design is most likely bound to end in frustration. G-seat somatic cues may be capable of enhancing the roll and yaw illusion, but not of inducing said illusions.

The situation is somewhat different regarding g-seat z-axis (vertical) acceleration cueing capabilities. Changes in z-axis acceleration can be produced by a variety of aircraft attitude or velocity changes, one of which is bank angle changes in a coordinated turn. This may partially explain the Task 2 performance improvement for the no-motion/g-seat/high-time group. Experienced pilots were apparently able to utilize g-seat z-axis cues to maintain a steady bank angle. As reported in reference 9, pilots generally approved of one type or another of g-seat z-axis acceleration cues.

As has been shown, the type of task affects the relative utility of g-seat and motion system cueing. It appears that tasks involving rapid and substantial changes in roll or yaw are best performed in a motion-based simulator without a g-seat, whereas those tasks composed of slow expected changes in bank angle, pitch, and z-axis velocities can be performed adequately by experienced pilots in either motion-based or g-seat-equipped simulators. A reminder, however, is that the preceding applies only to those simulators with a forward field-of-view visual display. The presence of a wide angle visual display may alter these findings.

The type of aircraft may also have a profound effect on the utility of g-seat versus motion-system cueing. Large-cabin aircraft typically are flown at constant altitude and airspeed with minimal changes in attitude, except for takeoff rotation, climb-out, flare, banking to exit the terminal area, or emergency maneuvers. Of these maneuvers, perhaps the flare and emergency maneuvers are the most critical to the safety of the flight. It may be possible to cue a flare maneuver using g-seat cueing; however, due to the design features of large-cabin aircraft, many emergency maneuvers, such as those in this study, involve rapid changes in aircraft bank, yaw, and cockpit lateral position, thus making g-seat cueing less appropriate than motion system cueing. Given the ability to use motion-system cueing to cue maneuvers like flare or takeoff rotation, it seems that on an overall basis, the most useful large-cabin aircraft simulator is a motion-equipped one.

CONCLUSIONS

1. Motion cueing improved performance, to some extent, on all three tasks.

2. The motion variable consistently accounted for far more performance variance than did the g-seat variable.

3. G-seats of the design used here are not recommended for use on large-cabin aircraft simulators.

4. Motion systems of the type simulated in this study are recommended for use on large-cabin aircraft simulators, especially for cueing maneuvers involving high-frequency, large-amplitude roll and yaw cues.

Ames Research Center
National Aeronautics and Space Administration
Moffett Field, California 94035, July 2, 1979

APPENDIX A

DESCRIPTION OF G-SEAT HARDWARE AND SOFTWARE DEVELOPMENT

HARDWARE DEVELOPMENT

The g-seat hardware was obtained from the Air Force Aeronautical Systems Division/ENCT, Wright-Patterson Air Force Base, Ohio; it was modified as necessary to meet the needs of this study.

The initial hardware was a full working set designed for use in a fighter-type seat. This set included the matrix of bellows for the seat pan, backrest, and thigh panels; the lap-belt drive mechanism; and an array of 30 servovalves and associated electronics to drive the lap-belt and bellows mechanisms. The basic pilot seat substructure was not provided with this initial set of hardware.

Because this study required a transport-type seat, the backrest structure was modified from the fighter-type to the transport-type. Additional modifications to the g-seat hardware were as follows:

1. Redesign of the lap-belt mechanism to reduce the force level, increase the travel capability, and provide additional over-force safety features.

2. Instrumentation added to the seat-pan, backrest, and lap-belt mechanisms to provide position information for calibration and testing purposes.

3. Modification of the servovalve electronics from a 10 V to 100 V system.

A photograph of the g-seat is presented in figure 2 and a schematic of the seat pan, backrest, thigh panels, and lap-belt arrangement is presented in figure 10.

Detailed performance measurements of the modified g-seat hardware were not obtained prior to its use in this study. However, a subsequent study, reported in reference 4, has shown the modified hardware to perform much like a first-order system with a time constant of 0.53 sec and a pure time delay of 0.083 sec. Frequency response data for this hardware are presented in figure 11.

DRIVE PHILOSOPHY AND SOFTWARE DEVELOPMENT

The software used to generate the drive signals for the g-seat was a modified version of the software obtained from the Air Force Human Resources Laboratory, Williams Air Force Base, Arizona. This original software package was a developmental version used to drive the fighter-type g-seat in the Advanced Simulator for Undergraduate Pilot Training (ASUPT) at Williams AFB and was based on the drive philosophy developed by Kron (ref. 1).

The basic structure of this software was not altered and is represented in block diagram form in figures 12 through 22. Since the structure of the software allows for a wide variation in drive philosophy, the modification from a fighter-type to transport-type drive and other changes required merely changing the values of parameters within the drive program.

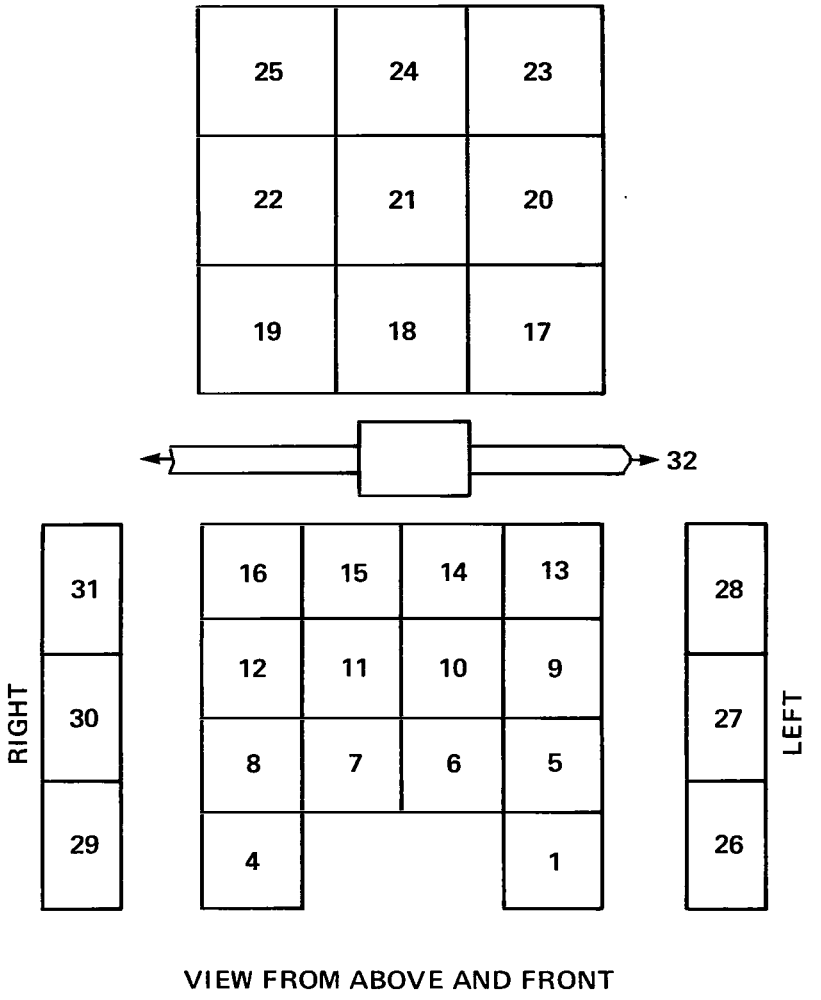

Figure 10.– Schematic of seat-pan, backrest, thigh-panels, and lap-belt arrangement.

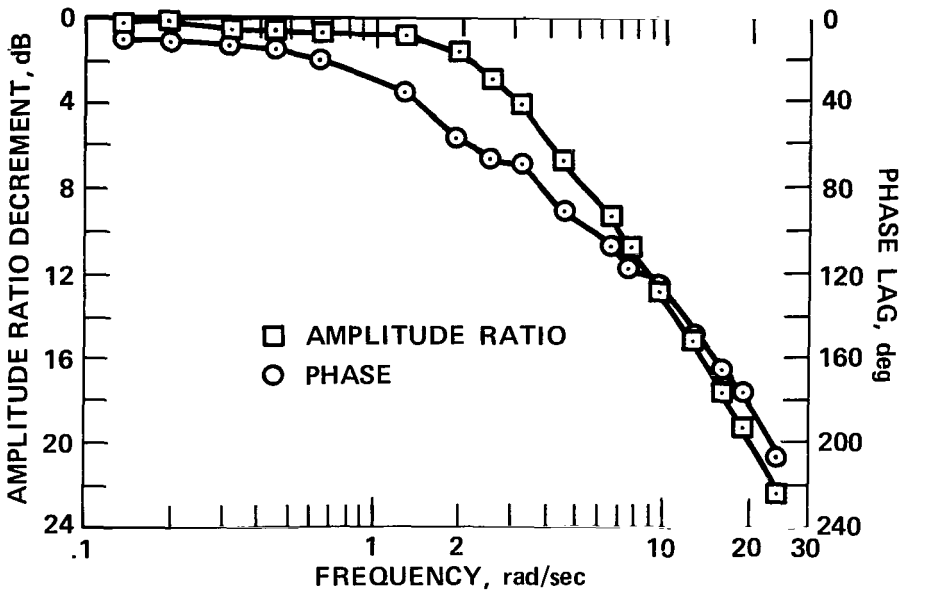

Figure 11.– G-seat frequency response characteristics.

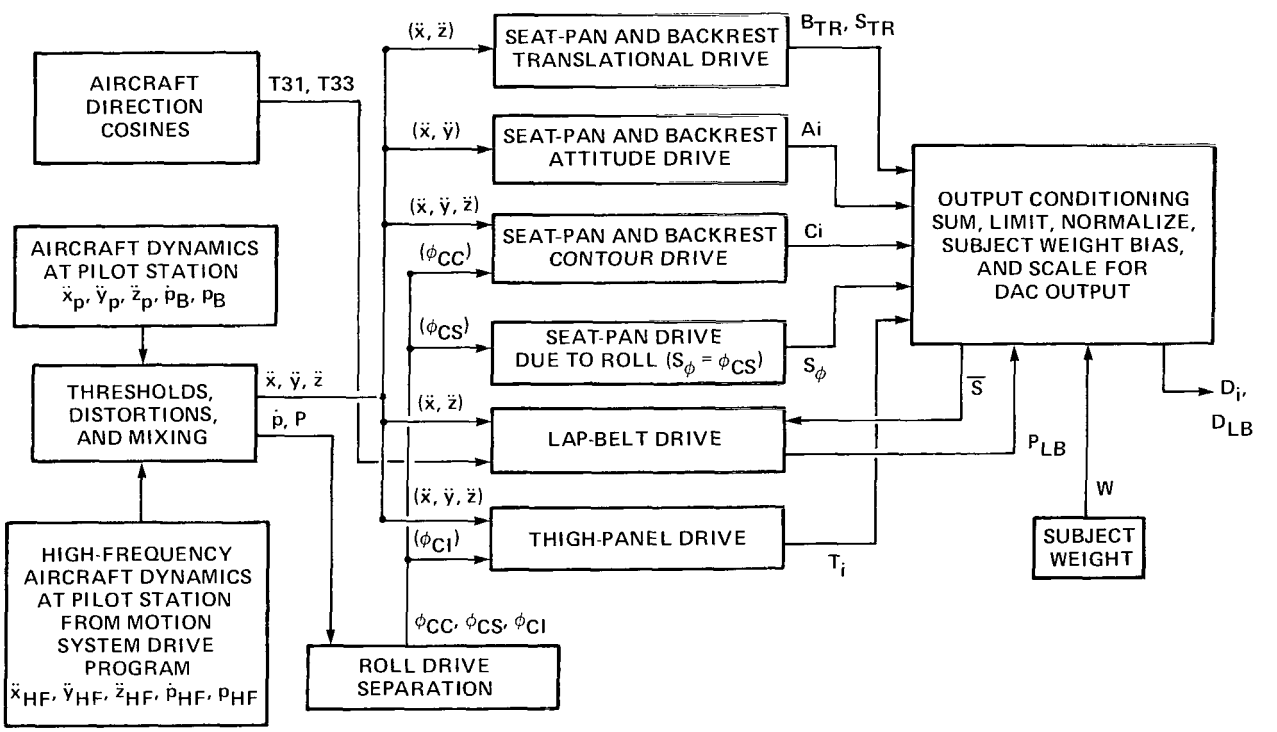

Figure 12.– G-seat drive program: functional block diagram.

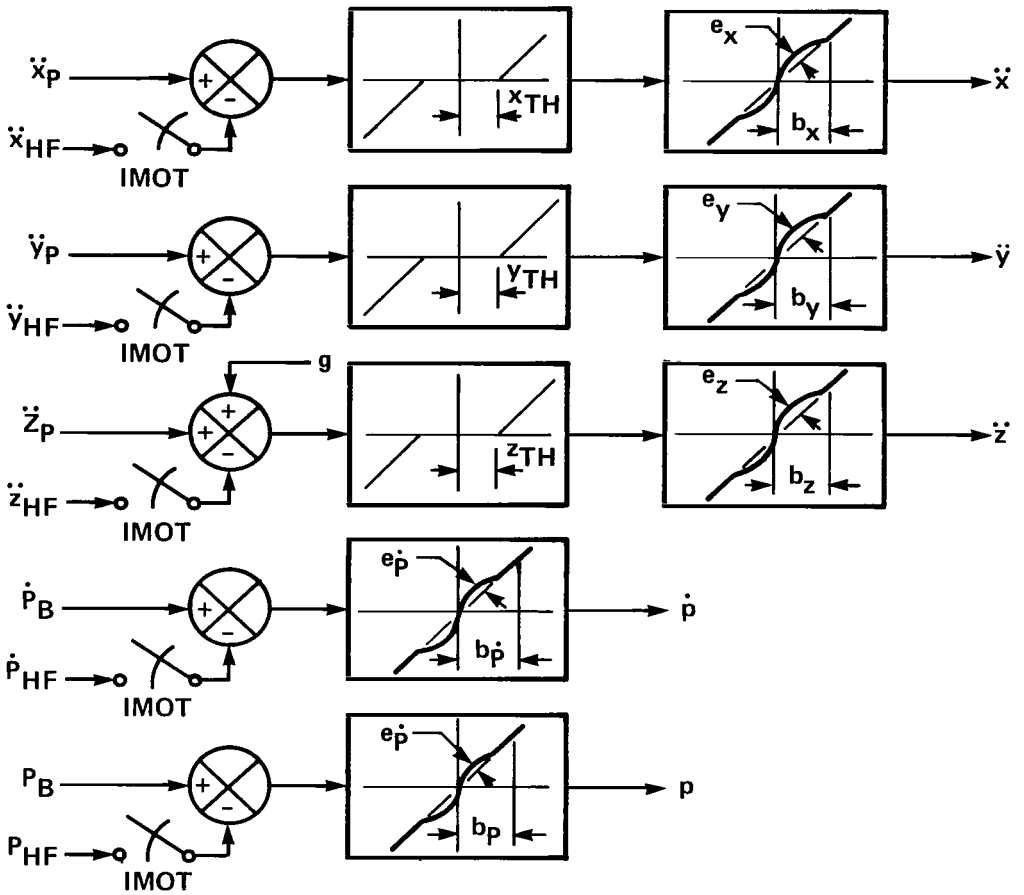

DISTORTION EQUATIONS

$$\text{FOR } |x_{IN}| \leq b;\ x_{OUT} = 1.4e\left[\frac{a}{b} + \sin\left(4.7\,\frac{a}{b}\right)\right] + x_{IN},$$

WHERE

$$a = e\left(1 - \left|\frac{x_{IN}}{b}\right|\right)\left(\frac{x_{IN}}{b} + \sin\left\{4.7\,\frac{x_{IN}}{b}\right\}\right) + x_{IN}$$

$$\text{FOR } |x_{IN}| > b;\ x_{OUT} = x_{IN}$$

Figure 13.– Thresholds, distortion, and mixing.

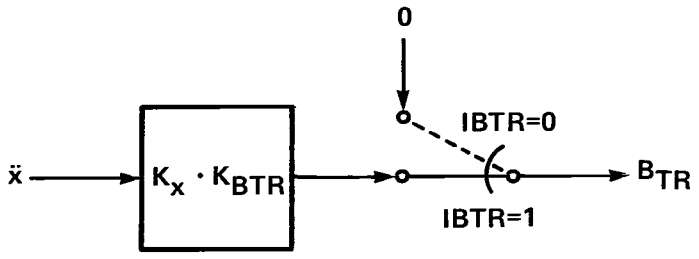

BACKREST TRANSLATIONAL DRIVE

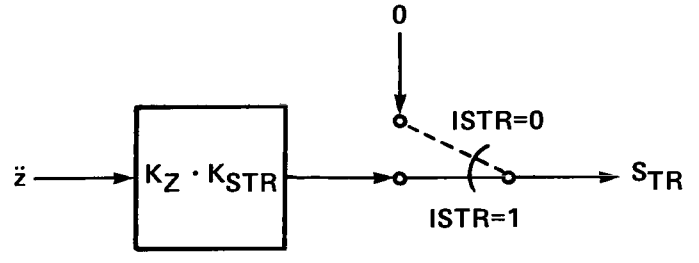

SEAT-PAN TRANSLATIONAL DRIVE

Figure 14.– Seat-pan and backrest translational drives.

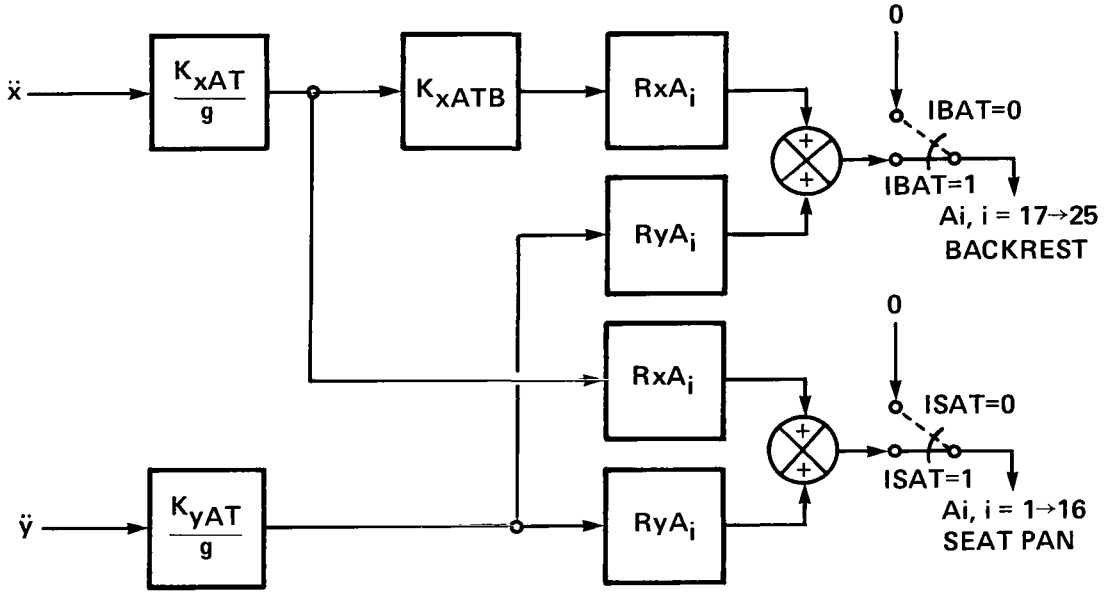

Figure 15.– Seat-pan and backrest attitude drives.

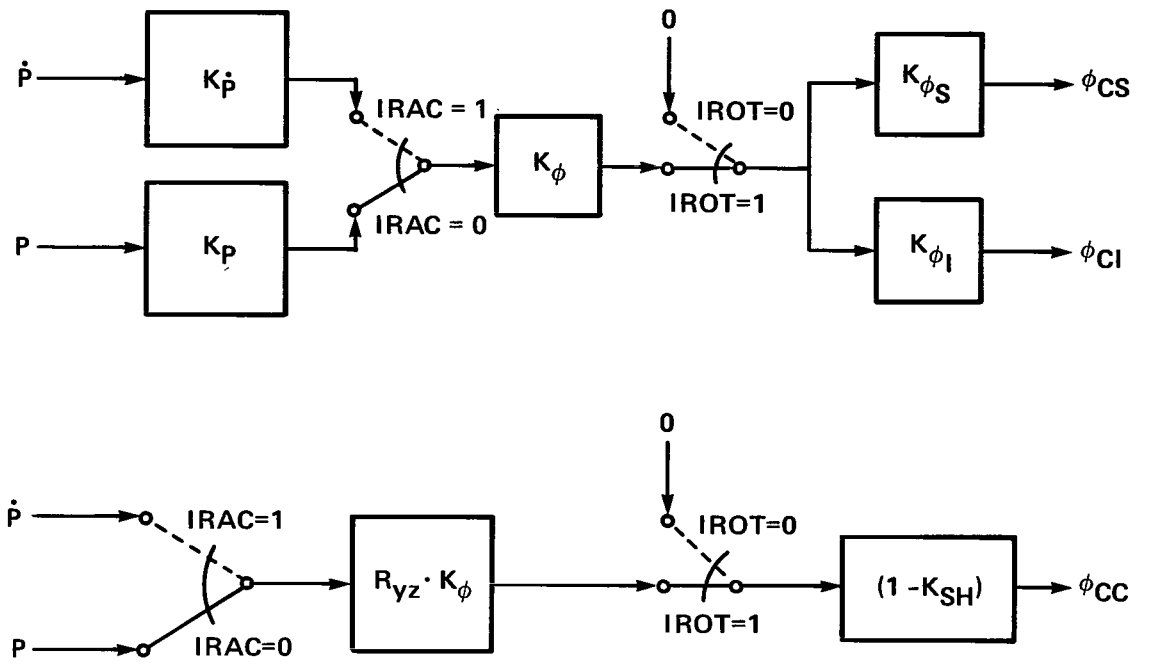

Figure 16.– Roll-drive separation.

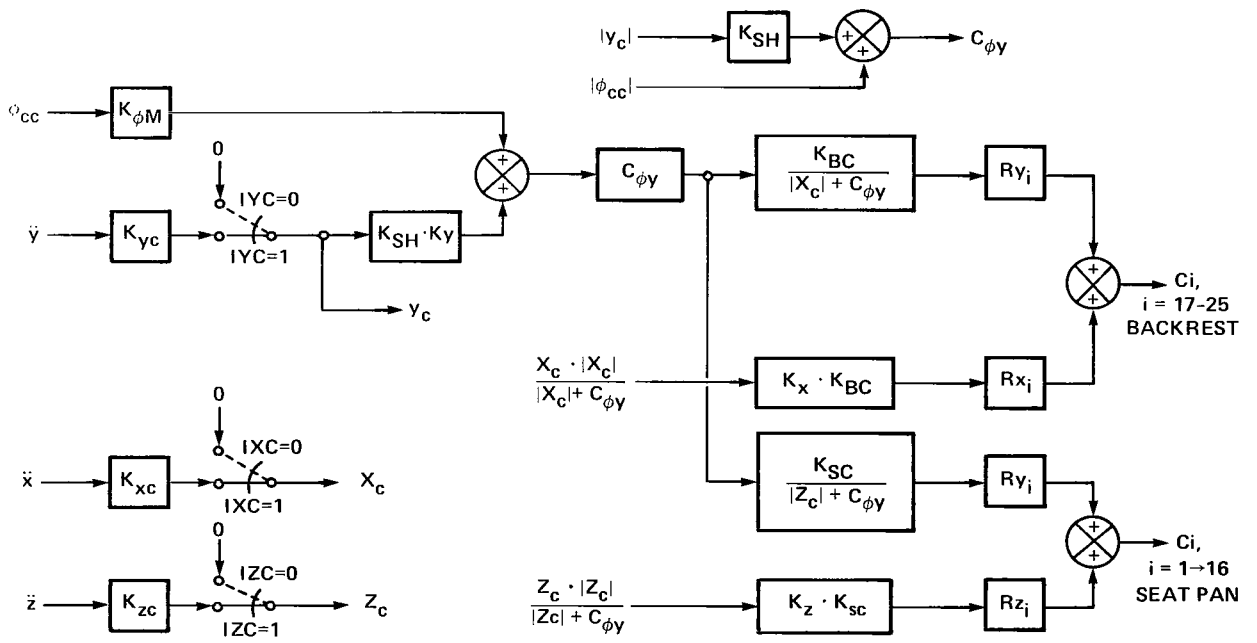

Figure 17.– Seat-pan and backrest contour drive.

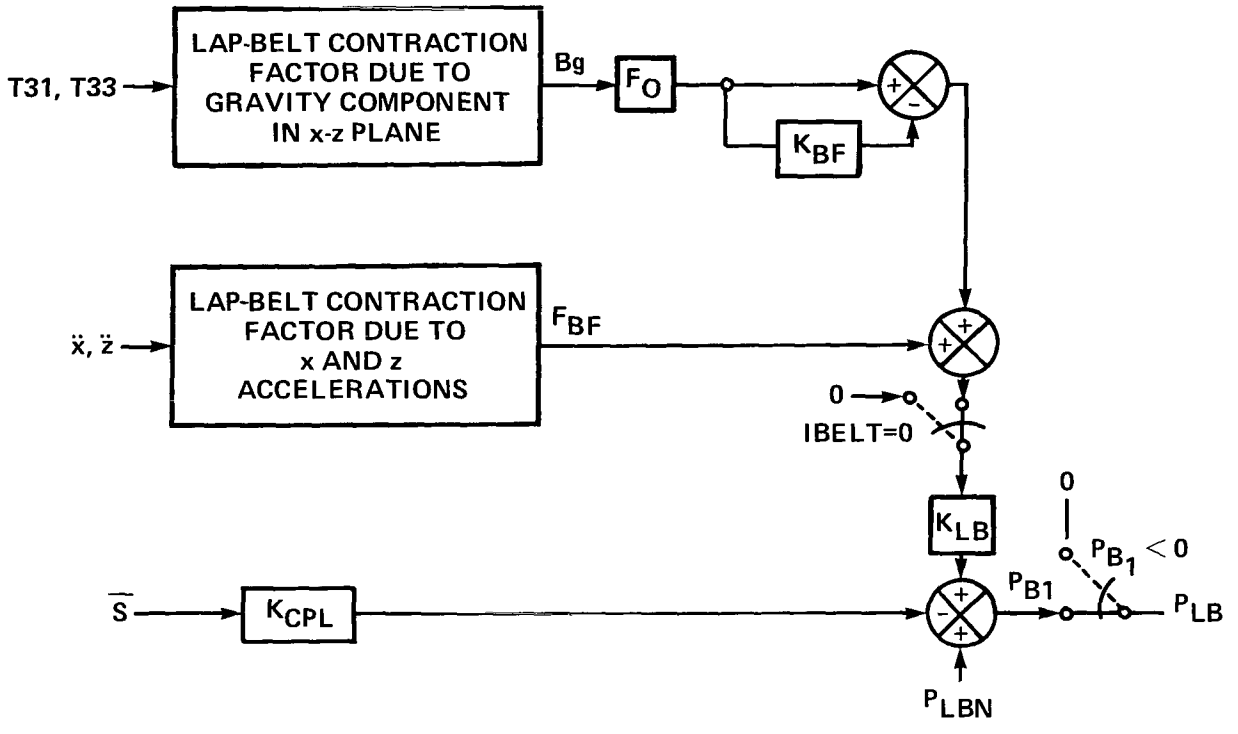

Figure 18.– Lap-belt drive.

$$Gx = g \cdot T31$$
$$Gz = g \cdot T33$$
$$Gxz = \sqrt{Gx^2 + Gz^2}$$

FOR $Gxz \neq 0$, AND,

- FOR $Gx < 0$ AND $Gz < 0$, $Bgf = Gz/Gxz$
- FOR $Gx \geqslant 0$ AND $Gz \geqslant 0$, $Bgf = 1 - Gz/Gxz$
- FOR $Gx \geqslant 0$ AND $Gz < 0$, $Bgf = 1$
- FOR $Gx < 0$ AND $Gz \geqslant 0$, $Bgf = 0$

FOR $Gxz = 0$, $Bgf = 0$

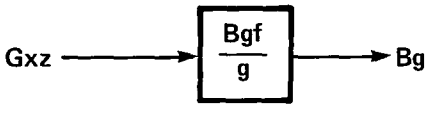

Figure 19.– Lap-belt contraction factor due to gravity component in x-z plane.

$$Fxz = \sqrt{\ddot{x}^2 + \ddot{z}^2}$$

FOR $Fxz \neq 0$ AND,

- FOR $\ddot{x} < 0$ AND $\ddot{z} < 0$, $B_{F_f} = (|\ddot{x}| - |\ddot{z}|)/Fxz$
- FOR $\ddot{x} \geqslant 0$ AND $\ddot{z} \geqslant 0$, $B_{F_f} = (|\ddot{z}| - |\ddot{x}|)/Fxz$
- FOR $\ddot{x} \geqslant 0$ AND $\ddot{z} < 0$, $B_{F_f} = -1$
- FOR $\ddot{x} < 0$ AND $\ddot{z} \geqslant 0$, $B_{F_f} = 1$

FOR $Fxz = 0$, $B_{F_f} = 0$

FOR $B_{F_f} \geqslant 0$, $B_F = K_{BF} \cdot F_o$

FOR $B_{F_f} < 0$, $B_F = B_{Fo}$

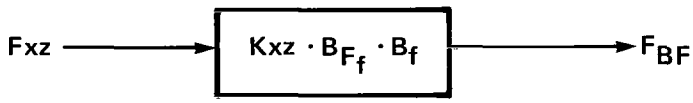

Figure 20.– Lap-belt contraction factor due to x and z accelerations.

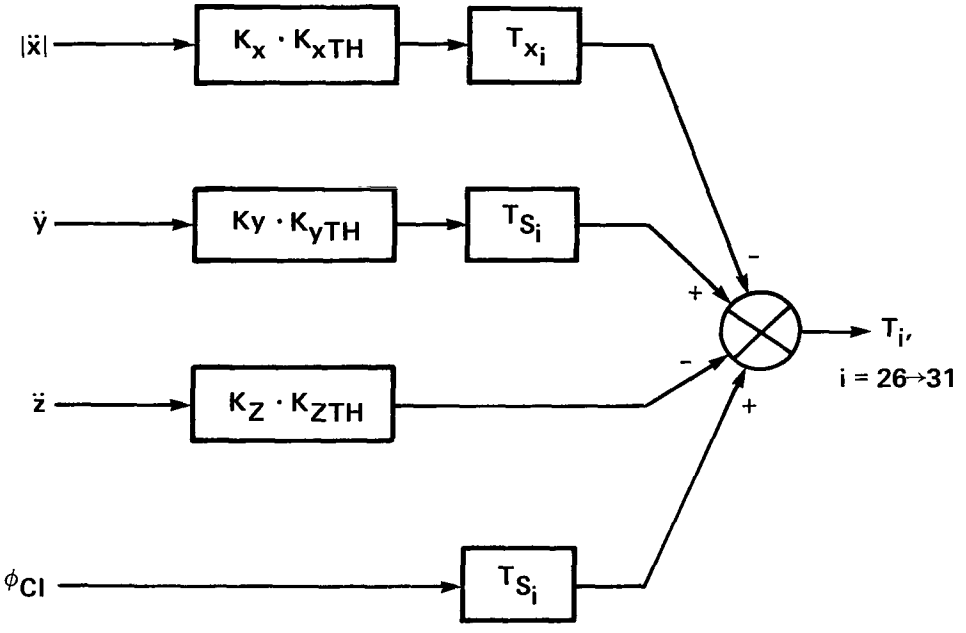

T_{x_i}, cm				T_{s_i}
i	$\ddot{x}>0$	$\ddot{x}<0$	$\ddot{x}=0$	
26	0	Xm	0	-1
27	Xn	Xn	0	-1
28	Xm	0	0	-1
29	0	Xm	0	1
30	Xn	Xn	0	1
31	Xm	0	0	1

$X_n = 11.75$ cm

$X_m = 23.50$ cm

Figure 21.– Thigh-panel drive.

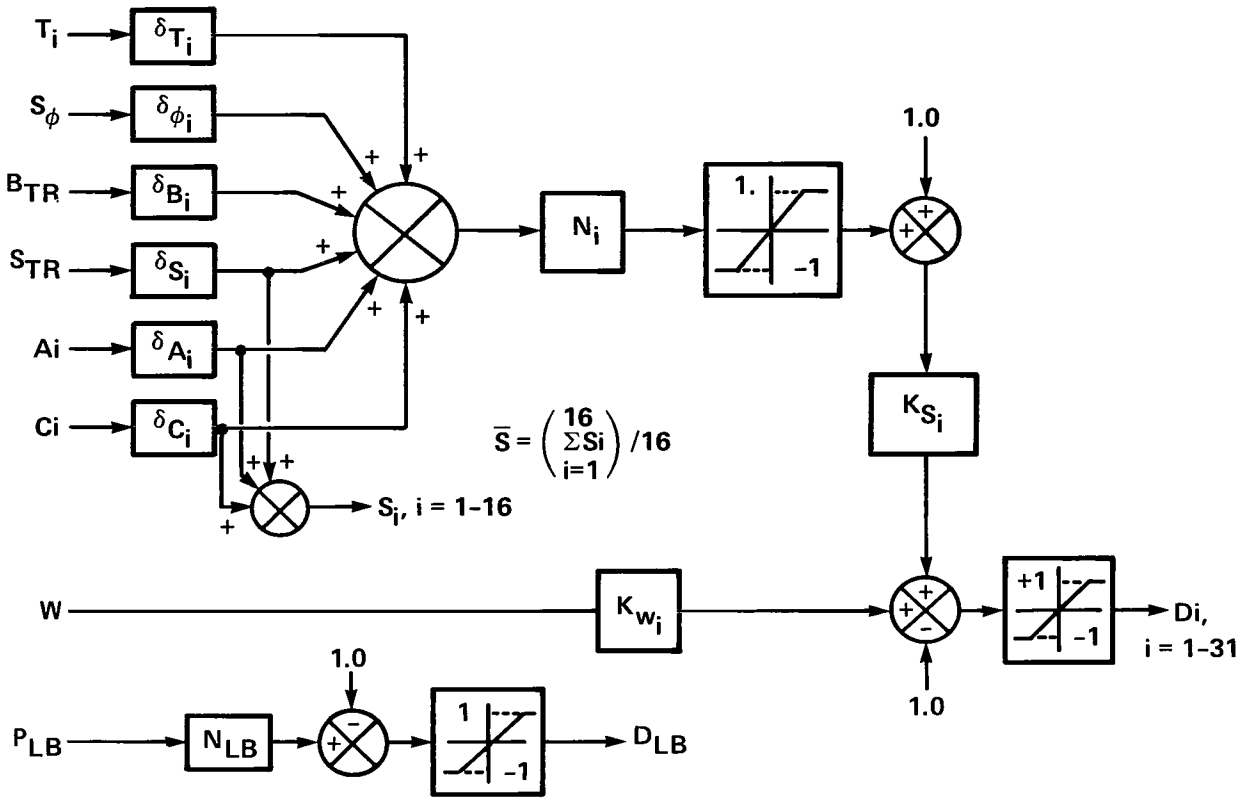

Figure 22.— Output conditioning.

Developmental testing was performed to determine the appropriate values of g-seat drive program parameters for the flight regimes treated in this study. This testing involved three Air Force pilots (two KC-135 instructor pilots and one pilot with a wide background in several aircraft types) and one NASA senior simulation engineer/pilot. Each of the pilots evaluated a broad range of drive program parameters for several flight tasks which included both longitudinal and lateral/directional modes of the aircraft.

The major gains, thresholds, belt-force gain, and shaping parameters were independently varied until a combination was achieved that the test pilots considered to best represent the aircraft for the flight regimes of interest. This method was used to evaluate both the g-seat-only configuration and the g-seat/motion-system combination. For the latter configuration, the dynamic input to the g-seat drive program was formed by subtracting the high-frequency portion of the aircraft dynamics (obtained from washout filters in the motion system drive program) from the total aircraft dynamics. Thus, in the combined system, the g-seat was driven with the low-frequency portion of the aircraft dynamics not directly produced by the motion system. When used alone, the total spectrum of aircraft dynamics was used as input to the g-seat drive program.

The full set of values of the g-seat drive program parameters used for this study are presented in tables 3 and 4. Reference to figures 10 and 12–22 should aid in the interpretation of these values.

TABLE 3.– G-SEAT DRIVE PARAMETER ARRAYS

i	R_{xA_i}	R_{yA_i}	R_{x_i}	R_{y_i}	R_{z_i}	N_i, cm^{-1}	K_{w_i}, $kg^{-1} \times 10^4$	K_{s_i}
1	0.95	-0.975	---	0	1.0	0.286	4.977	0.500
2	.95	-.325	---	0	0		3.646	.477
3	.95	.325	---	0	0		3.646	.472
4	.95	.975	---	0	1.0		4.977	.448
5	.32	-.975	---	0	1.0		25.811	.480
6	.32	-.325	---	.4	-1.0		7.292	.490
7	.32	.325	---	-.4	-1.0		7.292	.480
8	.32	.975	---	0	1.0		25.811	.462
9	-.32	-.975	---	0	1.0		29.746	.480
10	-.32	-.325	---	1.0	-1.0		69.446	.500
11	-.32	.325	---	-1.0	-1.0		69.446	.420
12	-.32	.975	---	0	1.0		29.746	.480
13	-.95	-.975	---	0	1.0		8.391	.430
14	-.95	-.325	---	0	-1.0		63.658	.500
15	-.95	.325	---	0	-1.0		63.658	.456
16	-.95	.975	---	0	1.0		8.391	.500
17	-.73	-.515	-1.0	0	---	.450	0	.625
18	-.73	0	1.0	0	---		122.687	.625
19	-.73	.515	-1.0	0	---		0	.625
20	0	-.515	-1.0	0	---		0	.625
21	0	0	0	0	---		61.344	.625
22	0	.515	-1.0	0	---		0	.625
23	.73	-.515	.7	.6	---		0	.320
24	.73	0	.3	0	---		0	.320
25	.73	.515	.7	-.6	---		0	.320
26	---	---	---	---	---	.394	9.276	.158
27	---	---	---	---	---		26.836	.158
28	---	---	---	---	---		37.203	.158
29	---	---	---	---	---		9.276	.158
30	---	---	---	---	---		26.836	.158
31	---	---	---	---	---		37.253	.158

TABLE 4.– G-SEAT DRIVE PARAMETERS

Parameter	Value used	Units
x_{TH}	0	cm/sec^2
y_{TH}	0	cm/sec^2
z_{TH}	0	cm/sec^2
e_x	15	cm/sec^2
e_y	13	cm/sec^2
e_z	35	cm/sec^2
$e_{\dot{p}}$	1.0	rad/sec^2
e_p	0.2	rad/sec
b_x	100	cm/sec^2
b_y	75	cm/sec^2
b_z	1000	cm/sec^2
$b_{\dot{p}}$	6.0	rad/sec^2
b_p	1.5	rad/sec
K_x	0.0267	dimensionless
K_y	0.0351	dimensionless
K_z	1.33×10^{-3}	dimensionless
K_{xz}	1.4815×10^{-3}	dimensionless
K_{BTR}	0.175	sec^2
K_{STR}	-0.875	sec^2
K_{XAT}	0.254	cm/g
K_{yAT}	2.159	cm/g
K_{xATB}	-1.0	dimensionless
$K_{\dot{p}}$	0.4233	cm sec^2/rad
K_p	1.27	cm sec/rad
K_ϕ	1.0	dimensionless
K_{ϕ_s}	0.5	dimensionless
K_{ϕ_I}	0.25	dimensionless
R_{yz}	94.44	cm
K_{SH}		
for $IYC = 1$	0.5	dimensionless
for $IYC = 0$	0.0	dimensionless
K_{ϕ_M}		
for $IRAC = 1$	0.00448	sec^2/rad
for $IRAC = 0$	0.01345	sec/rad
K_{xc}	-0.5	sec^2
K_{yc}	1.0	sec^2
K_{zc}	-1.0	sec^2
K_{BC}	-0.4	dimensionless
K_{SC}	0.75	dimensionless
K_{LB}	2,791.856	dyne/cm^2 kg
F_o	17.86	kg/cm/sec^2
K_{BF}	0.5	dimensionless

TABLE 4.– CONCLUDED

Parameter	Value used	Units
K_{CPL}	52,660.745	dyne/cm^3
P_{LBN}	313,711.46	dyne/cm^2
B_{F_o}	1.786	kg/cm/sec^2
K_{xTH}	0.0394	sec^2/cm
K_{yTH}	-0.7	sec^2
K_{zTH}	-1.0	sec^2
N_{LB}	1.902×10^{-6}	cm^2/dyne
δ_{T_i}		
for i = 1–25	0	dimensionless
for i = 26–31	1	dimensionless
δ_{ϕ_i}		
for i = 1, 5, 9, 13	1	dimensionless
for i = 4, 8, 12, 16	-1	dimensionless
otherwise	0	dimensionless
δ_{S_i}		
for i = 1–16	1	dimensionless
for i = 17–31	0	dimensionless
δ_{B_i}		
for i = 17–25	1	dimensionless
otherwise	0	dimensionless
δ_{A_i}		
for i = 1–25	1	dimensionless
for i = 26–31	0	dimensionless
δ_{C_i}		
for i = 1–25	1	dimensionless
for i = 26–31	0	dimensionless
IBTR	1	dimensionless
ISTR	1	dimensionless
IBAT	1	dimensionless
ISAT	1	dimensionless
IRAC	0	dimensionless
IROT	1	dimensionless
IXC	0	dimensionless
IYC	0	dimensionless
IZC	1	dimensionless
IBELT	1	dimensionless

APPENDIX B

DEFINITION OF WITHIN TASK CONDITIONS AND SEQUENCING

SEQUENCE OF TASKS AND CONDITIONS

During a typical daily training session, two pilots trained in 30-min shifts until both had completed training for all three tasks. The tasks were presented to each pilot in the order shown in table 5. The definitions of the task condition numbers are presented in tables 6 through 8.

TABLE 5.– SEQUENCE OF TASKS

Task	Condition
2	1–4
1	1, 2
3	1, 2
2	5–7
2	*a*
3	3–9
1	3–13
3	10
1	14
1	*a*
3	11
3	*a*

[a]Task sequence repeated until no noticeable improvement was indicated.

TABLE 6.– TASK 1 CONDITIONS

Condition	Outboard engine failed[a]	Altitude (above ground level) of failure, m (ft)	
1	R	122	(400)
2	L	91	(300)
3	L	152	(500)
4	R	91	(300)
5	L	46	(150)
6	L	30	(100)
7	L	76	(250)
8	R	61	(200)
9	R	46	(150)
10	L	152	(500)
11	R	91	(300)
12	L	46	(150)
13	L	30	(100)
14	R	61	(200)

[a]R = right, L = left.

TABLE 7.– TASK 2 CONDITIONS

Condition	Ascending turn[a]	Descending turn[a]
1	L	R
2	R	L
3	R	L
4	L	L
5	R	R
6	R	L
7	L	R

[a]R = right, L = left.

TABLE 8.– TASK 3 CONDITIONS

Condition	h_W, m (ft)	U_2, km/hr (knots)	U_1, km/hr (knots)	ψ_2, deg	ψ_1, deg
1	168 (550)	37 (20)	37 (20)	110	80
2	183 (600)	93 (50)	37 (20)	120	70
3	158 (520)	65 (35)	28 (15)	45	80
4	91 (300)	37 (20)	46 (25)	60	100
5	122 (400)	19 (10)	19 (10)	80	10
6	145 (475)	56 (30)	37 (20)	100	160
7	162 (530)	74 (40)	19 (10)	55	90
8	152 (500)	37 (20)	37 (20)	110	70
9	138 (450)	19 (10)	56 (30)	70	100
10	107 (350)	56 (30)	74 (40)	120	80
11	183 (600)	56 (30)	37 (20)	110	70

DEFINITION OF WIND SHEAR PARAMETERS

The approach for this landing task was on a 90° heading and began at an altitude of 304.8 m (1000 ft) with a mean wind of U_2 from a heading of ψ_2. The wind condition remained constant until an altitude of h_W was reached. From h_W down to 30.48 m (100 ft) below h_W, the mean wind velocity and/or heading were varied linearly to U_1 and ψ_1, respectively. These conditions were then held constant for the remainder of the landing. A moderate level of turbulence (an rms level equal to 10% of the mean wind) was maintained throughout the approach and landing.

REFERENCES

1. Kron, G. J.: Advanced Simulation in Undergraduate Pilot Training: G-Seat Development. Final Report for Period Mar. 1971–Mar. 1975, AFHRL-TR-75-59 (III), Oct. 1975.

2. Griffin, J.; McFarland, B.; and DeBerg, O. H.: Evaluation of G-Seat Cueing in Large Bodied Aircraft. Eighteenth Annual Conference of Military Testing Association Proceedings, Oct. 1976.

3. Bose, S. C.; Parris, B. L.: Simulation of a Synergistic Six-Post Motion System on the Flight Simulator for Advanced Aircraft at NASA-Ames. NASA CR-152010, 1977.

4. Showalter, T. W.; and Miller, R. J.: G-Seat Step Input and Sinusoidal Response Characteristics. NASA TM-78478, 1978.

5. Parris, B. L.; and Cook, A. M.: Effects of Visual and Motion Simulation Cueing Systems on Pilot Performance During Takeoffs With Engine Failures. NASA TP-1365, 1978.

6. Dixon, W. J.: BMDP-P4M Biomedical Computer Programs. University of California Press, Berkeley, Calif., 1975.

7. Dixon, W. J.: BMD-08U Biomedical Computer Programs. Second ed. University of California Press, Berkeley, Calif., 1968.

8. Lindquist, E. F.: Design and Analysis of Experiments in Psychology and Education. Houghton Mifflin, Boston, 1956.

9. Showalter, T. W.: A Pilot Evaluation of Two G-Seat Cueing Schemes. NASA TP-1255, 1978.

10. Sinacori, J. B.; Stapleford, R. L.; Jewell, W. F.; and Lehman, J. M.: Researchers Guide to the NASA-Ames Flight Simulator for Advanced Aircraft (FSAA). NASA CR-2875, 1977.

1. Report No.	2. Government Accession No.	3. Recipient's Catalog No.
NASA TP-1601		

4. Title and Subtitle

THE EFFECTS OF MOTION AND G-SEAT CUES ON PILOT SIMULATOR PERFORMANCE OF THREE PILOTING TASKS

5. Report Date: January 1980

6. Performing Organization Code:

7. Author(s)

Thomas W. Showalter and Benton L. Parris

8. Performing Organization Report No.: A-7875

9. Performing Organization Name and Address

Ames Research Center, NASA
Moffett Field, Calif. 94035

10. Work Unit No.: 505-09-41

11. Contract or Grant No.:

12. Sponsoring Agency Name and Address

National Aeronautics and Space Administration
Washington, D.C. 25046

13. Type of Report and Period Covered: Technical Paper

14. Sponsoring Agency Code:

15. Supplementary Notes

16. Abstract

Data are presented that show the effects of motion system cues, g-seat cues, and pilot experience on pilot performance during takeoffs with engine failures, during in-flight precision turns, and during landings with wind shear. Eight groups of USAF pilots flew a simulated KC-135 using four different cueing systems. The basic cueing system was a fixed-base type (no-motion cueing) with visual cueing. The other three systems were produced by the presence of either a motion system or a g-seat, or both. Extensive statistical analysis of the data was performed and representative performance means were examined. These data show that the addition of motion system cueing results in significant improvement in pilot performance for all three tasks; however, the use of g-seat cueing, either alone or in conjunction with the motion system, provides little if any performance improvement for these tasks and for this aircraft type.

17. Key Words (Suggested by Author(s))	18. Distribution Statement
Motion and g-seat cue evaluation Ground-based simulation Flight simulation Pilot performance in simulators	Unlimited STAR Category – 05

19. Security Classif. (of this report)	20. Security Classif. (of this page)	21. No. of Pages	22. Price*
Unclassified	Unclassified	45	$4.50

*For sale by the National Technical Information Service, Springfield, Virginia 22161

NASA-Langley, 1980

2 1 1U,A, 010780 S00903DS
DEPT OF THE AIR FORCE
AF WEAPONS LABORATORY
ATTN: TECHNICAL LIBRARY (SUL)
KIRTLAND AFB NM 87117